Prog. Oceanog. Vol. 22, pp. 125 - 170, 1989.
Printed in Great Britain.

0079 - 6611 / 89 $0.00 + .50

Circulation and hydrography of the Levantine Basin. Results of POEM coordinated experiments 1985-1986

E. Özsoy*, A. Hecht** and Ü. Ünlüata*

*Institute of Marine Sciences, Middle East Technical University, PK 28, Erdemli, Içel, 33731, Turkey

**Israel Oceanographic and Limnological Research Ltd., Tel Shikmona, POB 8030, Haifa, 31080 Israel

(*Submitted*: March 1988 *Revised Draft Accepted*: October 1988)

Abstract — A brief review of the meteorological setting, hydrography and the circulation in the Levantine Basin of the Eastern Mediterranean is given. The recent high resolution data obtained in POEM coordinated experiments of 1985-1986 are then used to optimally estimate the circulation in the basin in two different seasons and to describe the water mass distributions. Some of the features observed during the experiments support the historical knowledge on the locations of sub-basin scale gyres and the general circulation, in addition to which some new features are established. Details of the circulation such as the intensity, the multiple scales and the three dimensional structure of the various vortices and the Central Levantine Basin Current are displayed extensively. A variety of sub-basin, meso- and sub-mesoscale vortices occur with highly assymmetric (baroclinic) vertical structures. Some eddies split into multiple centres with depth, interpreted as indicating possible coalescences. A number of long-lived eddies were persistent in both surveys. The sub-surface Atlantic Water (AW) is advected by and entrapped within the eddy field. The Levantine Intermediate Water (LIW) at intermediate depths is shown to be maintained throughout the year in the northeastern sector of the Levantine Basin and along the periphery of the Rhodes gyre. The Levantine Intermediate Water also has a patchy distribution, owing to the advection and trapping by the eddy field which it helps to generate through adjustment processes.

CONTENTS

1. INTRODUCTION

The need for basic oceanographic experiments covering the Eastern Mediterranean (EM) extensively, and at the same time with sufficient resolution, have long been recognised in view of the insufficiency of historical data in the region. The scientific plans of the coordinated experiments to be reported here have been developed within the POEM (Physical Oceanography of the Eastern Mediterranean) Research Programme (UNESCO, 1984). Two major experiments were completed in October-November 1985 and March-April 1986 respectively, by various collaborating groups. We report on some results of these two coordinated surveys pertinent to the Levantine Sea, obtained and jointly analysed by Turkish and Israeli teams (respectively the IMS-METU and the IOLR). Complementary data from other parts of the Eastern Mediterranean held by other institutions are expected to contribute further information on the interactions with the other basins. The recent POEM coordinated activities have already begun changing some of the earlier concepts of the Eastern Mediterranean oceanography (reviewed in the following) and further analyses and modelling are expected to yield much improved understanding of its regional dynamics.

In the following we will refer to the October-November combined data set as ON85 and assume it represents the summer environment of the Levantine Basin since it coincided with the period of maximum heat storage in the region (e.g. Hecht *et al.*, 1985). In parallel, we will refer to the March-April 1986 combined data set as MA86 and assume that it represents the winter environment of the Levantine Basin since it coincided with the period of minimum heat storage in the region (e.g. Hecht *et al.*, 1985). Our reference to the seasons as such is based on the climatological characteristics of the region: the spring and autumn often occur as very short transition periods between the summer and winter which also come later than their continental counterparts, a property that has been widely utilized in the literature (e.g. Ovchinnikov, 1966).

A brief review of the regional characteristics is given in Section 2, followed by the description of the data acquisition in Section 3. The summer and winter circulation characteristics are described in Sections 4 and 5 respectively, and the hydrographic variability is discussed in Section 6. The quantitative distribution of bulk water properties are then given in Section 7. Discussion and conclusions are provided in Section 8. A description of the data processing and analysis methodology is provided in Appendices A + B.

2. REVIEW OF REGIONAL CHARACTERISTICS

2.1. *Bottom topography*

With a volume of 7.5 x 10 km the Levantine Basin is the second largest basin of the Eastern Mediterranean (Fig. 1). It is encircled by Asia Minor, the northeast African mainland and the Cretan Archipelago. Narrow passages (Straits of Rhodes, Scarpanto and Kasos) allow connection to the

Aegean Sea, and the connection to the Ionian Sea occurs through the Cretan Passage (south of Crete). The continental shelf is generally narrow (excluding the Gulf of Iskenderun and the Nile Fan), and the mid-basin depths are reached within 10-20km from the coast. The major troughs are at the Rhodes (4000m), Antalya (2000-2500m), Cilicia (1000m) and Lattakia (1000-1500m) Basins, the Hellenic Trench (3000-3500m) and the Herodotus Abyssal Plain (3000m). The latter two depressions are separated by the Mediterranean Ridge (2500m). The other features of elevated topography are at Anaximander Seamount (1500m) located between Rhodes and Antalya Basins, and Hecateus and Eratosthenes Seamounts (1000m) to the south of Cyprus. The Cilicia and Lattakia Basins to the north and east of Cyprus are relatively shallow compared to the rest of the Levantine Sea, and are connected by a narrow channel of 700m depth in the mid-portion of the sill extending from Cape Andreas (Cyprus) to Iskenderun. The Cilician Basin adjoins the Antalya Basin at a sharp depth transition from 1000m to 2000m just to the northeast of the western tip of Cyprus.

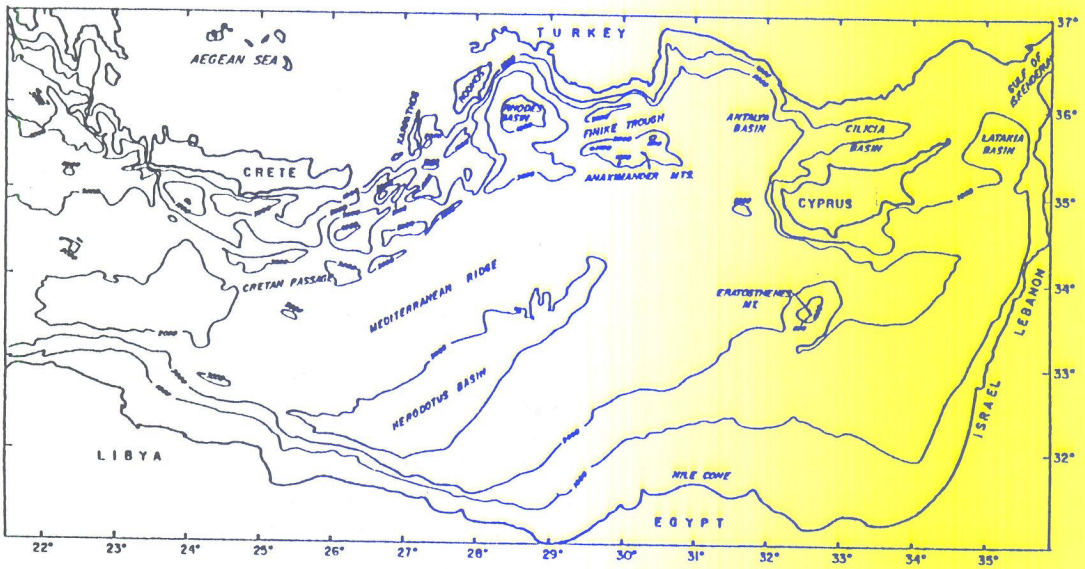

FIG.1. The bottom topography and geography of the Levantine Basin.

2.2. *Meteorology and surface fluxes*

The meteorology of the region displays extreme variability. Westerlies, Etesians and coastal seabreeze cells are the common wind systems in summer and autumn, while frequent extratropical cyclones and local wind regimes such as Poyraz and Sirocco winds characterize the winter and spring (REITER, 1975; MEDITERRANEAN PILOT, 1976; BRODY and NESTOR, 1980; ÖZSOY, 1981). In summer and early autumn, the westerlies are reinforced by the northerly Etesians in the southern Aegean (REPAPIS, ZEREFOS and TRITAKIS, 1987) with the resultant west-northwesterly winds sweeping over the Levantine Basin (BRODY and NESTOR, 1980; MIDDELANDSE ZEE, 1957).

In winter, roughly 30 of the 75 cyclones annually observed within the Mediterranean region are steered along the northern Levantine coasts and are rejuvenated there. Cyclones mostly arrive in the region from the Ionian Sea, but some come from north Africa (REITER, 1975; BRODY

and Nestor, 1980). After cyclonic passages, northerly cold, dry Poyraz winds are pumped through the gaps in the Taurus mountain along the Turkish coast (Özsoy, 1981), in addition to the northerly winds at the wide southern Aegean region.

In general these localised cold, dry outbreaks are expected to influence the oceanographic variability along the northern Levantine coast both in terms of the non-uniform wind distribution (curl of wind stress) and also through extensive evaporative heat and buoyancy losses. The latter have been recognised by Wüst (1961) and Morcos (1972) as the major source of Levantine Intermediate Water (LIW) formation in late winter. Lacombe and Tchernia (1974) have previously associated the regions of water mass formation within the Mediterranean with those of northerly cold outbreaks. Rapid cooling of coastal waters during such events have been reported by Özsoy and Ünlüata (1983), who showed that the stepwise winter cooling near the coast coincides with Poyraz events.

Along the southern coast of the Levantine Basin, north African depressions (about 15 annually) either move eastward or follow the pathway taken by other Eastern Mediterranean cyclones to the north (Reiter, 1975). They are often preceded in winter by the southerly Sirocco winds (Khamsin near Suez Canal) advecting warm, dry air masses from the north African/Arabian deserts, which become humid upon reaching the northern regions of the Levantine Basin (Brody and Nestor, 1980).

The climatological mean wind stress distributions of May (1982) show that the highest annual wind stress magnitude and its curl occurs in the Aegean Sea, with some influence in the adjoining regions of the Levantine Basin. The wind stress over the Levantine Basin is generally northwesterly, except in winter when the average direction becomes westerly. Only some of the local wind regimes such as the Mistral (in the western Mediterranean), Bora (in the Adriatic) and Etesians and Poyraz (in the eastern Mediterranean) survive in the climatological averages. The Etesian occurs as a northerly jet in the south Aegean region and therefore generates curl of wind stress with positive sign to the east of its main axis (maximum near Rhodes) and of negative sign on its west (west of Crete), through most of the year excluding the winter). Computations made by Navarra (1986), based on larger data sets, confirm these essential features.

Although limited work appears to be done on the other climatological surface fluxes, fundamental estimates are provided by Bunker (1972), Bunker, Charnock and Goldsmith (1982), Colacino and Del'osso (1975, 1977), Bethoux (1979, 1980) and Peixoto, Almeida, Rosen and Salstein (1982), which point to large deficits of heat and buoyancy in the Eastern Mediterranean and especially in the northern Levantine Basin.

2.3. *Hydrography*

One of the most important water masses found in the Eastern Mediterranean is the Levantine Intermediate Water, which affects not only the entire Mediterranean, but the Atlantic Ocean as well (e.g. Arhan, 1987). The scatter in the T-S characteristics of LIW suggests the existence of a multiplicity of sources (Morcos, 1972) within the Levantine Basin, and the homogeneity (mixing) achieved further west indicates (Hopkins, 1978) its transit time is sufficiently long enough to render the LIW "stale" (Ovchinnikov, 1984) by the time it leaks out of the Levantine Basin. Little is known on the mechanisms responsible for LIW formation, except that the process has been linked to the evaporative losses of heat and buoyancy and mixing in the northern Levantine Basin (Wüst, 1961; Morcos, 1972) which result in cooling and increased salinity of surface waters in winter, generating motions limited to intermediate depths in early spring. Because of the assumed winter formation of Levantine Intermediate Water in the northern

and Nestor, 1980). After cyclonic passages, northerly cold, dry Poyraz winds are pumped through the gaps in the Taurus mountain along the Turkish coast (Özsoy, 1981), in addition to the northerly winds at the wide southern Aegean region.

In general these localised cold, dry outbreaks are expected to influence the oceanographic variability along the northern Levantine coast both in terms of the non-uniform wind distribution (curl of wind stress) and also through extensive evaporative heat and buoyancy losses. The latter have been recognised by Wüst (1961) and Morcos (1972) as the major source of Levantine Intermediate Water (LIW) formation in late winter. Lacombe and Tchernia (1974) have previously associated the regions of water mass formation within the Mediterranean with those of northerly cold outbreaks. Rapid cooling of coastal waters during such events have been reported by Özsoy and Ünlüata (1983), who showed that the stepwise winter cooling near the coast coincides with Poyraz events.

Along the southern coast of the Levantine Basin, north African depressions (about 15 annually) either move eastward or follow the pathway taken by other Eastern Mediterranean cyclones to the north (Reiter, 1975). They are often preceded in winter by the southerly Sirocco winds (Khamsin near Suez Canal) advecting warm, dry air masses from the north African/Arabian deserts, which become humid upon reaching the northern regions of the Levantine Basin (Brody and Nestor, 1980).

The climatological mean wind stress distributions of May (1982) show that the highest annual wind stress magnitude and its curl occurs in the Aegean Sea, with some influence in the adjoining regions of the Levantine Basin. The wind stress over the Levantine Basin is generally northwesterly, except in winter when the average direction becomes westerly. Only some of the local wind regimes such as the Mistral (in the western Mediterranean), Bora (in the Adriatic) and Etesians and Poyraz (in the eastern Mediterranean) survive in the climatological averages. The Etesian occurs as a northerly jet in the south Aegean region and therefore generates curl of wind stress with positive sign to the east of its main axis (maximum near Rhodes) and of negative sign on its west (west of Crete), through most of the year excluding the winter). Computations made by Navarra (1986), based on larger data sets, confirm these essential features.

Although limited work appears to be done on the other climatological surface fluxes, fundamental estimates are provided by Bunker (1972), Bunker, Charnock and Goldsmith (1982), Colacino and Del'osso (1975, 1977), Bethoux (1979, 1980) and Peixoto, Almeida, Rosen and Salstein (1982), which point to large deficits of heat and buoyancy in the Eastern Mediterranean and especially in the northern Levantine Basin.

2.3. *Hydrography*

One of the most important water masses found in the Eastern Mediterranean is the Levantine Intermediate Water, which affects not only the entire Mediterranean, but the Atlantic Ocean as well (e.g. Arhan, 1987). The scatter in the T-S characteristics of LIW suggests the existence of a multiplicity of sources (Morcos, 1972) within the Levantine Basin, and the homogeneity (mixing) achieved further west indicates (Hopkins, 1978) its transit time is sufficiently long enough to render the LIW "stale" (Ovchinnikov, 1984) by the time it leaks out of the Levantine Basin. Little is known on the mechanisms responsible for LIW formation, except that the process has been linked to the evaporative losses of heat and buoyancy and mixing in the northern Levantine Basin (Wüst, 1961; Morcos, 1972) which result in cooling and increased salinity of surface waters in winter, generating motions limited to intermediate depths in early spring. Because of the assumed winter formation of Levantine Intermediate Water in the northern

Levantine, its flow out of the Strait of Sicily has been described as being weaker in summer by WÜST (1961), but other investigators (KATZ, 1972) have found no seasonal dependence of the outflow, suggesting that LIW formation is either maintained continuously throughout the year or that it is formed in winter and released slowly and steadily during the whole year (HECHT, 1986).

OVCHINNIKOV (1984) relates LIW formation to the doming of cold, low salinity waters at the centre of the Rhodes cyclonic gyre, which then become even colder and gain salinity under the influence of winter conditions. Consequently the new water type undergoes radial, almost isopycnal sinking at the periphery and is arrested at intermediate depths; a model of this mechanism has been presented by OVCHINNIKOV and PLAKHIN (1984). It is, therefore, natural to find LIW mainly in anticyclonic eddies at the periphery of the Rhodes gyre or between the cyclonic eddies and the coast, where the isopycnic sinking should be intercepted. The results of the detailed study by ÖZTURGUT (1976) in winter, also provides evidence for this mechanism (ÜNLÜATA, 1986), although it seems that the results were not interpreted by ÖZTURGUT (1976) in the same way. An important consequence of the studies of ÖZTURGUT (1976) and OVCHINNIKOV, 1984) is that they strongly link LIW formation to meso-scale processes. Rapid changes in the existing patterns, sharp fronts and jets as well as smaller scale oscillatory features found in ÖZTURGUT (1976) point to energetic processes in the region. In fact, the presence of distinct gyres in the Levantine Basin contrasts strongly with a mean thermohaline circulation envisaged by the much criticized (OVCHINNIKOV, 1965) core method of WÜST (1961), and emphasises the importance of meso-scale turbulent stirring by the vortices as pointed out by MOSKALENKO (1974).

The second important water mass in the Eastern Mediteranean is the Atlantic Water (AW) which enters through the Gibraltar Strait to balance the mass deficit of the Mediterranean. It generally hugs the north African coast (LACOMBE and TCHERNIA , 1960, 1974; OREN, 1971) en-route to the Eastern Mediterranean (bypassing the Gulf of Tunis/Sidra), its salinity and depth range increases as it flows eastwards. In summer, the AW is overtopped by a surface mixed layer of higher temperature and salinity, so that it is identified by a subsurface salinity minimum (LACOMBE and TCHERNIA , 1960; OREN, 1971; MORCOS, 1972). The penetration of AW into the Levantine Sea increases during those summers when its inflow through the Gibraltar and Sicilian Strait is a maximum as a result of the increased mass deficits and the westerly winds (LACOMBE and TCHERNIA , 1960; ZORE-ARMANDA, 1969; OVCHINNIKOV, 1979). In winter, the presence of AW in the Levantine is often reduced as a result of increased mixing, reduced inflow through Sicily Strait and also its flow diverging from the north African coast and being deflected north towards Crete (OVCHINNIKOV, 1966). The divergence of AW from the north African coast may result from either the influence of cyclonic eddies (OVCHINNIKOV, 1966; HOPKINS, 1978) or the influence of the southerly Sirocco wind regime which develops when the Etesians cease (OREN, 1971; HOPKINS, 1978). However, these are generalizations drawn up in the absence of sufficient data and so conflicting situations can occur because of interannual and meso-scale variability. For example, ROSENTROUB, BISHOP and HECHT (1985) provide extensive data which indicate that at the time of the observations there was considerable penetration of AW into the southeastern Levantine in winter. This data contrast with those of MORCOS (1972) and MORCOS and HASSAN (1976) which showed northerly deflections of AW and its complete mixing down to 300m in winter and early spring, coinciding with the presence of Levantine Intermediate Water in the southern Levantine Basin. The mean properties, and various aspects of the water masses in the southeastern Levantine Basin can be found in HECHT, PINARDI and ROBINSON (1988).

The origin and the formation of the Eastern Mediterranean deep waters are poorly understood and since we will not be presenting directly related results, little purpose will be served by a review on this topic.

2.4. *Circulation*

It has been established for a long time that the dominant system is a basin-wide cyclonic mean circulation following the mainland coasts of the Levant (Nielsen, 1912; Schott, 1915; Wüst, 1961; Lacombe and Tchernia, 1974) and further studies have shown numerous cyclonic and anticyclonic sub-basin scale gyres occur within this general circulation (Ovchinnikov, 1966; Engel, 1967; Moskalenko, 1974 and Gerges, 1977). Ovchinnikov (1966) and Gerges (1977) found that the intermediate depth circulation essentially follows that of the surface but that the intensities of the gyres diminish with depth, some even disappear completely at the greater depths and no flow reversals are found. Below 500m, a basin-scale cyclonic circulation is established, as also pointed out by Wüst(1961) and more recently by El-Gindy and El-Din (1985).

The relative importance of topography, wind stress forcing, thermohaline driving forces, source/sink distribution at the Straits and internal mixing in determining the general circulation pattern are still to be determined to any reasonable level of confidence. According to Ovchinnikov (1966), Moskalenko (1974) and Menzin and Moskalenko (1982) the basic transport is wind driven, although thermohaline and baroclinic processes, bottom topography and β-effect seemed to them to play important roles in determining the details of the circulation. Gerges (1977) and Dzhioyev and Drozdov (1977) on the other hand, on the basis of the circulation being mainly cyclonic at all depths, concluded that the thermohaline gradients were the main driving force especially in the Levantine Basin and that wind drift components contributed only 30% to the circulation. Grillaki and Piaczek (1985) compared the relative roles of the influx from the Sicilian Strait and the wind stress distribution, and concluded that the wind stress driving is the more dominant of the two processes. The diversity of opinions arises from the different assumptions in the models or dynamic method calculations used, a review of which is provided by Malanotte-Rizzoli (1986) and Malanotte-Rizzoli and Hecht (1988).

To date, the most detailed description of the major features of the eastern Mediterranean circulation is by Ovchinnikov and Fedoseyev (1965), Ovchinnikov (1966) and Ovchinnikov *et al.* (1976), who based their computations mainly on data collected by Russian ships.

The calculations of Ovchinnikov and Fedoseyev (1965) reproduced many details of Eastern Mediterranean Circulation: One of the features noted by them was the Cyrenaican reversing gyre southwest of Crete (also found by Moskalenko, 1974; and Menzin and Moskalenko, 1982), which is cyclonic in the winter, reverses its sense in the summer and merges with the Ionian gyre to become a major anticyclonic gyre. The seasonal reversal of the Cyrenaica gyre appears to induce a seasonal reversal of the currents in the northern section of the Cretan Passage; thus the currents there are described as westward in the winter and eastward in the summer. The later monograph (Ovchinnikov *et al.*, 1976) is less decisive on the reversal of the Ionian Sea gyre and appears to depict the currents in the northern Cretan Passage as westward in the summer as well as in the winter. Ovchinnikov and Fedoseyev (1965) also described the anticyclonic southwestern Levantine gyre — southeast of Crete (see also Moskalenko, 1974; Dzhioyev and Drozdov , 1977; and Grillaki and Piaczek, 1985); the cyclonic Rhodes gyre — a quasi-permanent feature described in all of the investigations quoted above as well as in Özturgut (1976), Philippe and Harang (1982), and Anati (1984); and a weak cyclonic gyre in the southeastern Levantine Basin. Moreover, they described the route of the north African current — first from the Ionian Sea towards Cyrenaica (see also the satellite images of Philippe and Harang , 1982; as well as of Parmiggiani, Pinardi and Vivanti, 1986), then to the eastern tip of Crete, and on towards the mid Levantine Basin where it bifurcates. There, part of the waters turn counterclockwise west of Cyprus to become incorporated into the Rhodes gyre and part of them

flow eastward south of Cyprus (ENGEL, 1967) to join the Asia Minor current which meanders along the Anatolian coast. The vertical coherence and the mainly cyclonic sense of the circulation in the Levantine Basin, coupled with a return flow found solely in the deeper layers of the Ionian Sea led OVCHINNIKOV (1966) to conjecture that there must be intensive downwelling on the periphery of cyclonic gyres and along the shores of the Basin in order to compensate for the ascending motions within the cyclonic (divergence) zones.

The relatively small Rossby radius of deformation (about 15km — see ROBINSON, FELIKS and PINARDI, 1983) leads one to believe that superimposed on the sub-basin scale circulation, there must be meso-scale and sub-mesoscale features, i.e. eddies, jets, filaments and fronts. Fine resolution measurement and careful analysis have indeed confirmed the presence of such features (ÖZTURGUT, 1976; PINARDI, ROBINSON and HECHT, 1986; ÖZSOY, SAYDAM , SALİHOĞLU and ÜNLÜATA, 1986; ROBINSON, HECHT, PINARDI, BISHOP, LESLIE, ROSENTROUB, MARIANO and BRENNER, 1987; and HECHT, PINARDI and ROBINSON, 1988). Moreover, as pointed out by TZIPERMAN and HECHT (1987), there are indications of significant temporal variability of the sub-mesoscale features.

Unfortunately, the very few direct current meter measurements for the Basin consisted of short-term studies (see HECHT, 1986; MALANOTTE-RIZZOLI and HECHT, 1987). OVCHINNIKOV (1965) and OVCHINNIKOV and PLAKHIN (1965) reported on some daily measurements carried out in the Kasos Strait as well as in the Cretan Passage. However, their report does not seem to make a clear distinction between directly measured currents and computed geostrophic currents. ACCERBONI and GRANCINI (1972) reported on GEK measurements in the Kasos and Rhodes Straits as well as in the Cretan Passage. The only open water current measurements are due to GUIBOUT (1972). Using supplementary hydrographic data (DKSHOD, 1969), ÖZSOY, LATİF , OĞUZ and SAYDAM (1986a,b) have shown a general qualitative agreement of those current measurements and the geostrophic currents computed from objectively analysed data.

Very few long term current measurements have been made in the Levantine Basin. ÜNLÜATA, ÖZSOY and LATİF (1980), ÜNLÜATA, OĞUZ and ÖZSOY (1983) and ÖZSOY and ÜNLÜATA(1983), observed mean westerly currents on the order of 10 cm s^{-1} along the Turkish coast, which were superimposed on long term oscillatory trapped motions of the Cilician Basin (topographic Rossby waves, ÜNLÜATA, 1982) and subject to topographic steering and blocking along the rugged coast (ÜNLÜATA, OĞUZ and ÖZSOY, 1983).

3. DATA ACQUISITION

The POEM coordinated field experiments consisted of a series of quasi-simultaneous cruises during which the ships of the participating institutions acquired oceanographic data on a regular 0.5° (latitude and longitude) grid of stations covering almost the entire eastern Mediterranean (UNESCO, 1984).

Within this programme the R/V *Shikmona*, of the Israel Oceanographic and Limnological Research Ltd., occupied the stations south of 34° 15'N, and the R/V *Bilim*, of the Institute of Marine Sciences - Middle East Technical University, occupied the stations north of that latitude (Figs 2a,b). Periodically, both ships had to depart from the regular grid and change the intervals between some of the stations (Figs 2a,b). Typically, each vessel completed its survey within two to three weeks, but logistic constraints prevented the cruises being conducted simultaneously so that there was an interval of about 10 to 15 days between the cruises of the two ships. The combined survey of ON85 consisted of a total of 134 stations, while that of MA86 consisted of 107 stations.

The 0.5° spacing of the stations was inadequate for the resolution of small scale features, but

(a)

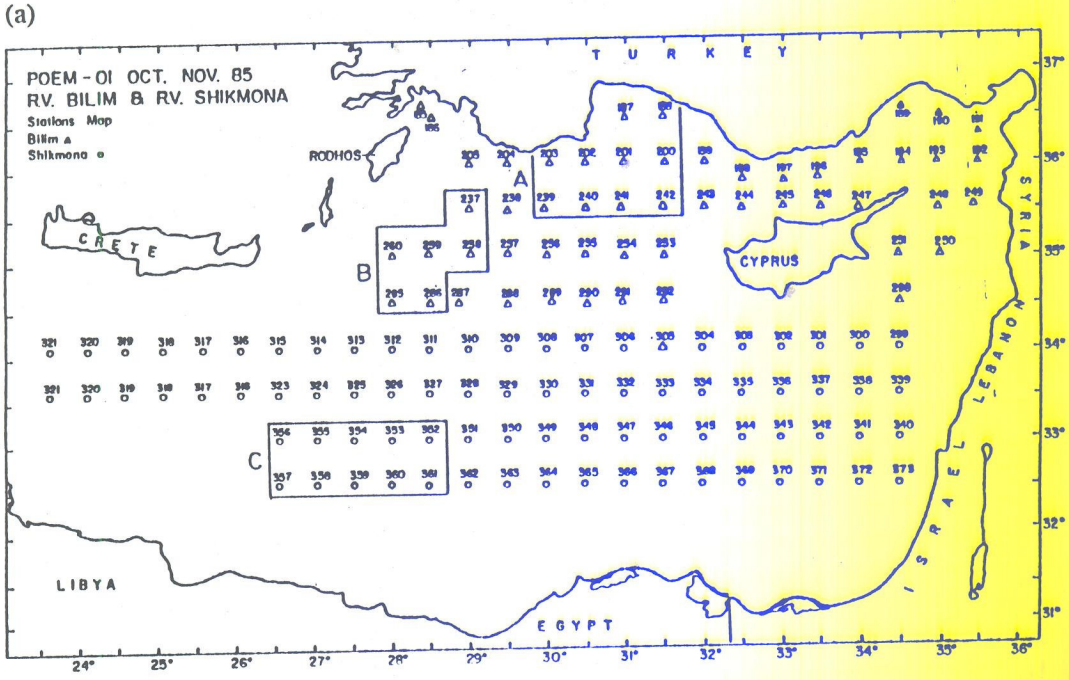

(b)

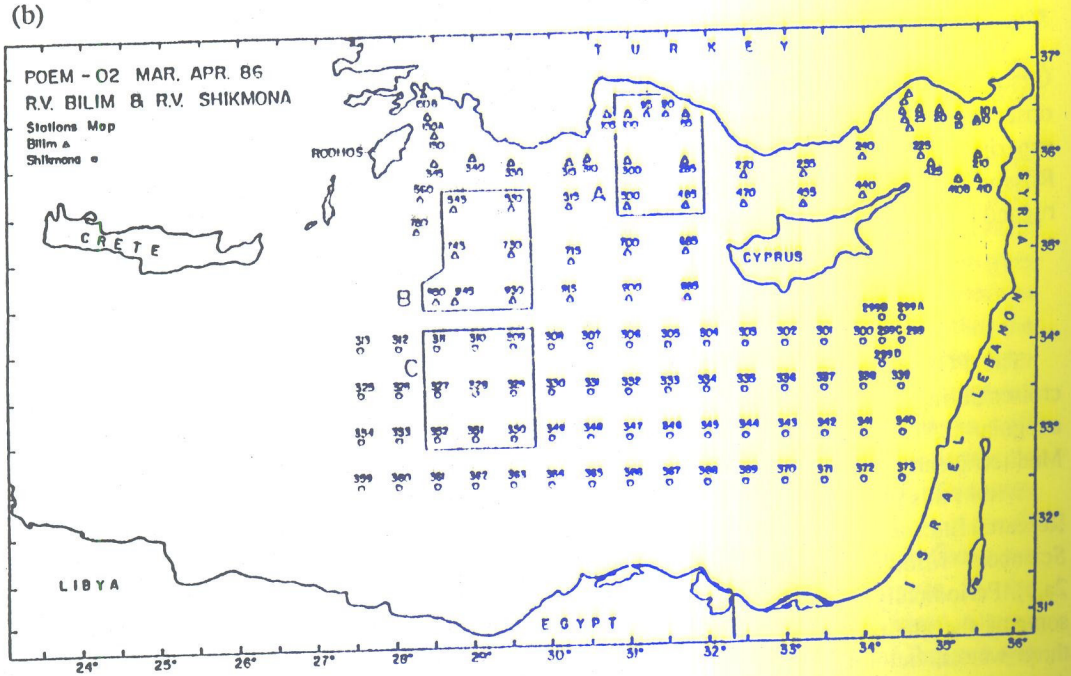

FIG.2a,b. Positions of the Stations occupied by the R/V *Bilim* and R/V *Shikmona* during the cruises of (a) October - November 1985 (ON85) and (b) March - April 1986 (MA86).

was a logistic compromise between the speed and the range of the ships, and the perceived needs to cover a large region and to approach synoptic sampling as close as possible. During the MA86 cruise the R/V *Bilim* tried out 0.75° zonal by 0.5° meridional station intervals.

The observations were made using the high resolution CTD systems of Neil Brown (NB-CTD) on the R/V *Shikmona* and SBE Model 9 (SBE-CTD) on the R/V *Bilim*. The SBE-CTD was also equipped with an oxygen sensor. The NB-CTD was lowered at a rate of 0.7-1.0 ms^{-1} and it sampled at a rate of 30 Hz. The SBE-CTD was lowered at a rate of 0.5-0.8 ms^{-1} and it sampled at a rate of 24 Hz. Thus both ships obtained data down to at least 1000m at intervals of the order of a few centimetres. The R/V *Shikmona* obtained additional data down to 2000m at every third station on its route as well as densely spaced XBT data between the five stations east of 32°30'E (the high density combination of XBT and CTD data were described and discussed in Robinson *et al.*, 1987).

4. THE SUMMER CIRCULATION

The topography of the surface geopotential anomaly (Fig.3a) in the summer reveals: (a) a cyclonic eddy in the Cretan Passage, (b) a large scale cyclonic eddy southeast of Rhodes — the Rhodes gyre — and its extension towards Cyprus, (c) a major anticyclonic gyre of almost equal size, north of Mersa Matruh, in the southwestern Levantine — the Mersa Matruh gyre — and, between them, (d) an intense jet with current velocities of the order of 40 cm s^{-1} (and perhaps even higher, in view of the smoothing performed by the objective analysis). This jet bifurcates and one of its branches flows northward around the Rhodes gyre. There, part of its waters penetrates into the Aegean Sea through the Strait of Rhodes, while the rest flows southward along the Cretan Archipelago and possibly westward through the northern section of the Cretan Passage. The other branch of this jet flows eastward where it bifurcates again with one branch turning northward west of Cyprus and the other branch turning southward south of Cyprus. Paucity of data (cf. Figs 2a and A1) prevents us from determining either the precise path or the proportional distribution of the fluxes of the jet's last two branches. Moreover, the jet's extension to the west is also poorly defined, since we do not have the necessary information along the Libyan coast and the eddy in the Cretan Passage was determined on the basis of too few stations (Figs 2a and A1). In the eastern Levantine Basin, south of Cyprus and west of Tel Shikmona, there appears to be another large anticyclonic gyre — the Shikmona gyre — containing three small scale anticyclonic eddies. This gyre directs the flow southward along the coast of Israel and then westward along the Egyptian coast. This section of the flow is also poorly determined because of the lack of stations at the crucial points along the Egyptian coast. We observed another cyclonic eddy east of Cyprus and a row of three anticyclonic eddies north of Cyprus and in the Cilician Basin which extended into the Antalya Basin. These features are separated from the easterly extension of the Rhodes gyre by the branch of the jet which encircles the gyre.

The cyclonic Rhodes gyre is a well known persistent feature (cf. Section 2) covering a large area centered upon the Rhodes Basin. It is often detected in satellite infrared images (Philippe and Harang, 1982; Satmer, from 1983 onward). At its centre is a doming of the cold isotherms with nearly uniform properties which indicates permanent upwelling. The dome appears more prominently in summer (Anati, 1984), which is to be expected in view of the increased wind stress curl associated with the eastern flank of the Etesian regime (cf. Section 2), and the subsequent surface divergence as described by Ovchinnikov (1966). On the other hand, the coincidence of the Rhodes cyclonic gyre with the Rhodes Basin depression, coupled with an anticyclonic eddy coinciding with the peak of the Anaximander Mountains immediately to the east (Fig.1) suggests there is topographical control (steady-state potential vorticity conservation).

(a)

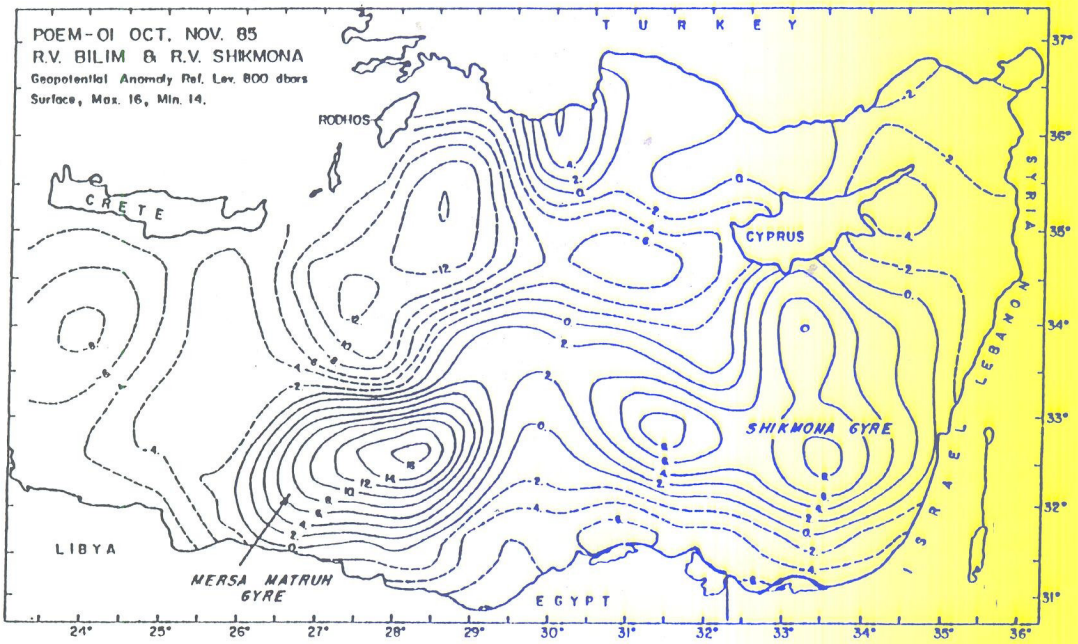

(b)

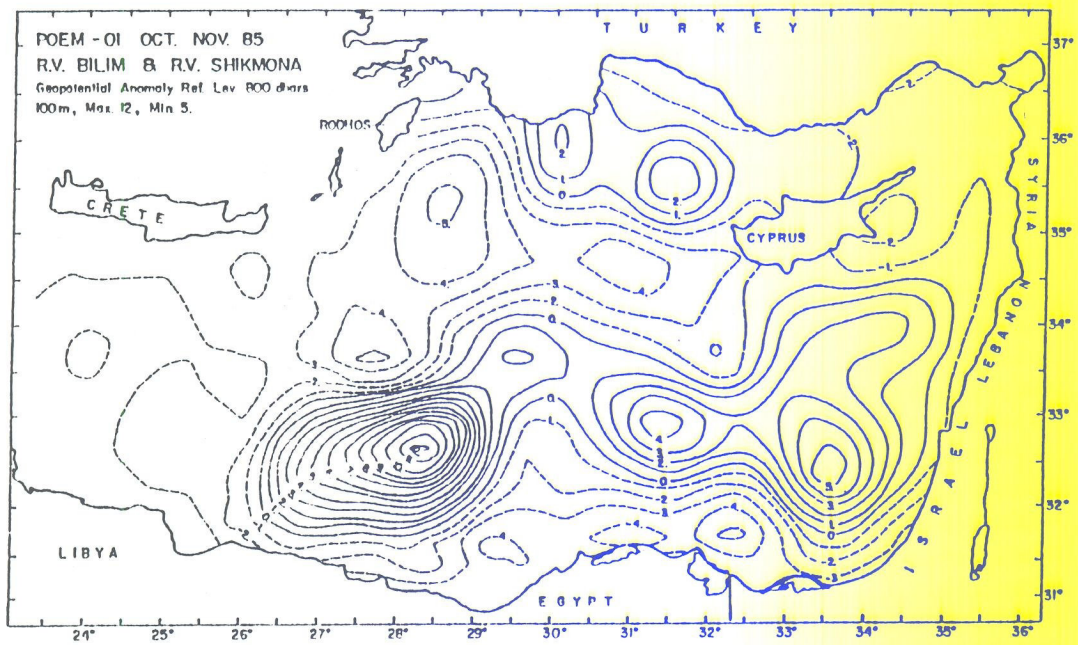

Fig.3a,b,c,d,e. Objective analysis of the geopotential anomaly of (a) the surface, (b) 100, (c) 200, (d) 300 and (e) 600dbar surfaces (relative to 800dbar) based on the combined ON85 data. (In these and the following figures the dynamic topography is given in units of cm, calculated relative to a reference level of 800 dbars, and a gradient of 1cm in 100km corresponds to a current speed of approximately 1cm s^{-1}).

(c)

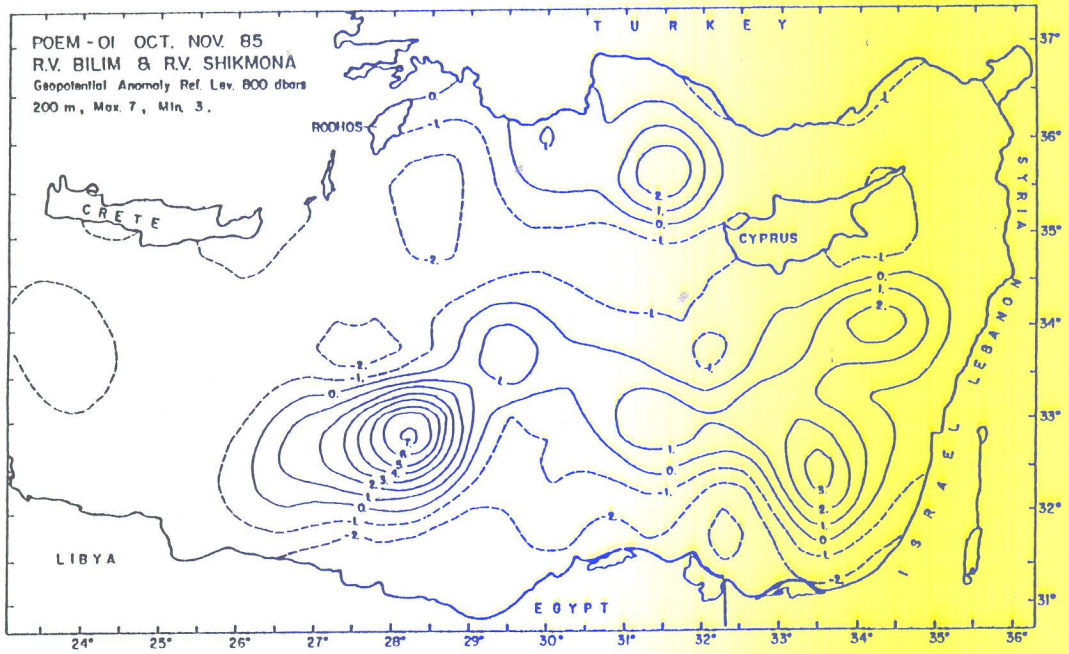

(d)

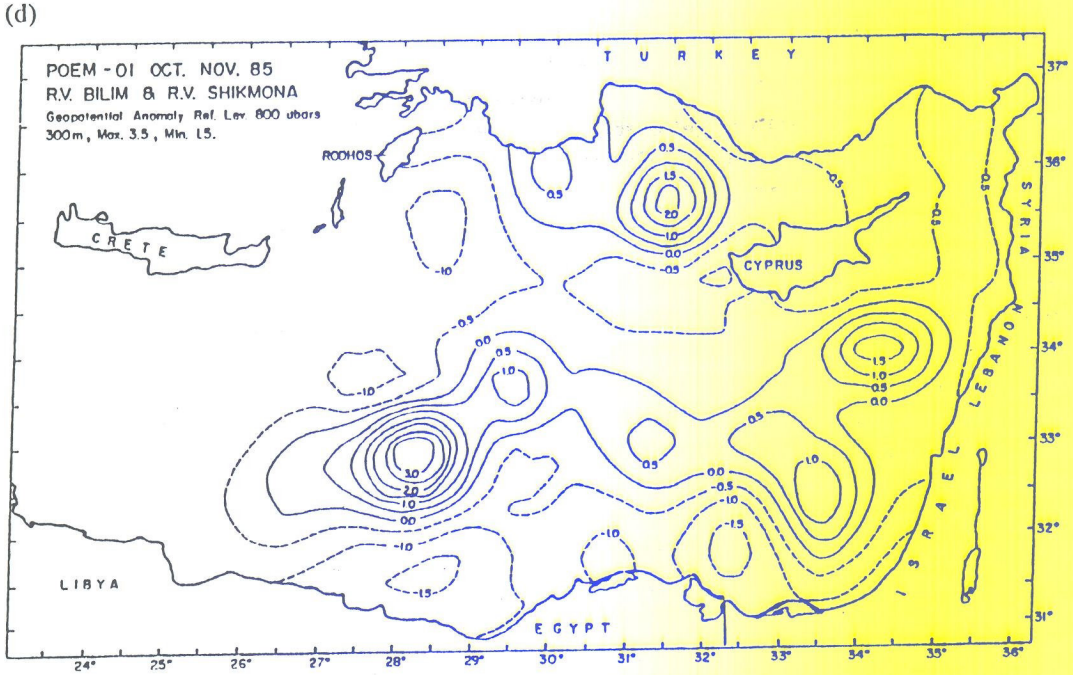

FIG. 3. Continued.

(e)

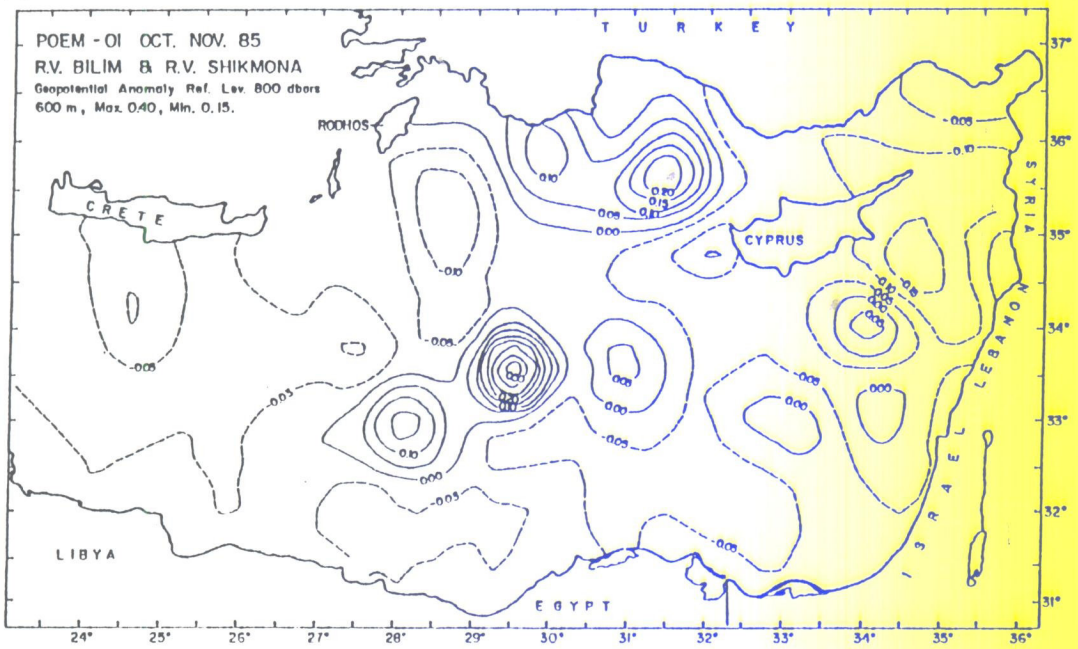

FIG. 3. Continued.

Based upon an analysis of the scales of motion of the Rhodes gyre, ANATI (1984) has estimated the ratio of available potential energy to the baroclinic component of kinetic energy APE/KE = $O(S^{-1}) \cong 50$, where $S = (R/L)^2$ is the stratification parameter of PEDLOSKY (1979) defined in terms of the internal Rossby radius of deformation R and the horizontal length scale L. Since $S<<0(1)$, the gyre is in the baroclinic instability range, but the release of energy in such large horizontal scales is very inefficient (PEDLOSKY, 1979). The energy ratio computed for the whole northern Levantine Basin was similarly found to be about APE/KE $\cong$ 20, based upon a calculation made from objectively analyzed fields of two earlier data sets (ÖZSOY *et al.*, 1986a,b). On the other hand, energy conversion is most efficient on scales comparable to the Rossby radius ($S=0(1)$), so that such motions should also be expected in the Levantine Basin. Indeed, surface temperature and salinity maps constructed from continuous on board sampling of seawater by ÖZTURGUT (1976) and also during the ON85 experiment (ÖZSOY, SAYDAM, SALİHOĞLU and ÜNLÜATA, 1986) show many fine structure details (fronts, filaments, fluctuations, eddies) superimposed on the larger scale surface signature of the meso-scale gyres and eddies. Satellite surface temperature data obtained during the ON85 experiment by PARMIGGIANI *et al.* (1986) definitively support the presence of these multiple scales of motion. High resolution sampling has indicated the presence of motions with $S=0(1)$ in other parts of the Levantine Basin (ROBINSON *et al.*, 1987).

The Central Levantine Basin Current (CLBC) which is the mid-latitude jet between the Rhodes and the Mersa Matruh gyres and its westward and eastward extensions, is depicted in both, the summer and the winter surface circulation maps of OVCHINNIKOV and FEDOSEYEV (1965), and can be assumed to be the continuation of the north African Current.

The main differences between the descriptions of the surface circulation in summer given by OVCHINNIKOV and FEDOSEYEV (1965) and our interpretations occur at the extremities of the Basin. However, the maps produced by OVCHINNIKOV and FEDOSEYEV (1965) are composites of the data from different cruises conducted years apart in which neither timing nor the distribution of the

various stations are clearly described (e.g. Ovchinnikov, 1965, 1966). On the other hand, at the western end of the Basin our data are neither sufficient nor detailed enough to resolve these discrepancies.

At the western end of the Basin, the Ovchinnikov and Fedoseyev (1965) map shows the waters flowing eastward through the northern section of the Cretan Passage in the opposite direction to the current we depict. Ovchinnikov (1965) presents the results of the October 1963 sixth R/V *Vavilov* cruise, which carried out detailed measurements in the Cretan Passage. The combination of geostrophic computations and direct current measurements (his fig.3) appear to indicate that, in the northern section of the Cretan Passage, the currents are flowing westward. Dynamic computations of the data acquired by the R/V *Bannock* in August 1967 (Mosetti, Accerboni and Lavenia, 1972) also show westward currents in the northern section of the Cretan Passage. Moreover, the GEK measurements made by Accerboni and Grancini (1972) in the surface layers of the Cretan Passage in September 1968 showed eastward flow in the northern section of the Passage, whereas their geostrophic computations show westward flow at the same location. It is interesting to note that for the rest of the Passage their geostrophic computations agreed fairly well with their GEK measurements. Finally, the summer surface circulation of Ovchinnikov *et al.* (1976) appears to indicate westward flowing currents in the northern Cretan Passage. Therefore, we may conclude that in the summer the westward flowing current in the northern section of the Cretan Passage is well established. Also at the western end of the Basin, where the Ovchinnikov and Fedoseyev (1965) summer circulation maps depict a cyclonic gyre, we found the large conspicuous Mersa Matruh anticyclonic gyre.

At the eastern end, in complete contradiction to our results, but in agreement with the traditional Nielsen (1912) description, the Ovchinnikov and Fedoseyev (1965) map indicates that most of the transport is eastward and counterclockwise around Cyprus, with almost no southward flow along the Israeli coast. Engel (1967) appears to be the first to contradict previous studies and to present computed anticyclonic geostrophic flow in the southeastern Levantine Basin. The observation of patches of AW which appear to be trapped in the southeastern section of the Levantine Basin (Rosentroub, Bishop and Hecht, 1985) also supports this interpretation. Engel (1967) also noted the blocking effect of the sill northeast of Cyprus (see Section 2), which may be responsible for the weakness and meandering of the Asia Minor Current. Pinardi, Robinson and Hecht (1986) indicate the occurrence of an anticyclonic eddy topographically locked over the Eratosthenes Seamount with cyclonic vortices forming in its lee. ON85 data for the same region augmented with numerous XBTs were studied by Robinson *et al.* (1987) and were shown to contain a complex pattern of small synoptic/mesoscale eddies, filaments and jets which mark the dispersion zone of the CLBC (or the North African Current). Analysis of earlier data sets indicates persistent anticyclonic eddies occur in this region (Feliks and Itzikowitz, 1967; Hecht *et al.* 1988). Therefore, one can consider the Shikmona anticyclonic gyre a well established feature of the summer circulation of the region.

The series of eddies in the Antalya and Cilician Basins mask the cyclonic mean flow around Cyprus (i.e. the Asia Minor current). Therefore, this current often appears as a meandering flow through this channel, and seems to be weaker than the jet flow on the southwestern side of Cyprus.

Finally, the surface circulation in Fig. 3a is in general agreement with the Ovchinnikov (1966) notion of anticyclonic gyres lying south of the detached north African current and cyclonic gyres to its north. The anticyclonic eddies in the northern Levantine Basin seem to be trapped between the cyclonic circulations and the coast.

The general features of the circulation do not change significantly down to about 50m. At 100m (Fig.3b) both the Mersa Matruh gyre and the central eddy of the Gulf of Antalya appear to

intensify, and the cyclonic gyres are generally weakened and shifted eastwards. Deeper down, this trend becomes more pronounced (Figs 3c, d and e). The Mersa Matruh gyre begins to split into two smaller eddies at 200db, of which the northeastern eddy becomes the dominant at 600db. At this level the surviving eddies are the remnants of the Mersa Matruh gyre, the anticyclonic eddies in the Gulf of Antalya and the one southeast of Cyprus, while the cyclonic eddies tend to have disintegrated.

The subsurface summer circulation maps of Ovchinnikov and Fedoseyev (1965) also show some gyres and eddies. However, the differences between their maps and ours are quite substantial. At 250db the only resemblance to our maps is the presence of the Rhodes gyre. Otherwise they depict cyclonic gyres at both of the locations where we find the Mersa Matruh and the Shikmona anticyclonic gyres. They also depict a sharply defined cyclonic current around Cyprus where we found nothing of the sort. For 500db the Ovchinnikov and Fedoseyev (1965) map is a weaker repetition of the 250db map and repeats the discrepancies between their map and ours.

5. THE WINTER CIRCULATION

During the MA86 cruises, both vessels were unable to occupy as many stations as in the summer ones (Fig.2b).

Also, the R/V *Bilim* experimented with longer zonal spacing between the stations. These factors are reflected in the error distribution map of the objective analysis of the data (Fig. A2b). Although the winter cruises were carried out some 4 to 5 months later than the summer ones, there is a striking consistency in some of the main circulation features, i.e. the Rhodes gyre, the Mersa Matruh gyre, and the Shikmona gyre could all be readily identified in the geopotential anomaly maps for all levels (Figs 4a-e). There are also some obvious differences. During the summer period, we have seen that at increasing depth the Mersa Matruh gyre appears to split into two smaller gyres of which the northeastern cell becomes the more intensive. During the winter period the same pattern emerges but at 600 dbar the southeastern Mersa Matruh gyre has degenerated completely.

A similar pattern emerged in the southeastern Levantine Basin, where during the summer we had distinguished three anticyclonic eddies (embedded in the Shikmona gyre) and where our results indicated that their remnants persisted during the winter. However, there appears to have been a shift in intensity northeastward and eventually, at a depth of 600 dbar, only the most northern eddy has survived. One is sorely tempted not to regard these eddies as individual entities that undergo some *in situ* transformation but as a single train of dynamic features extending from Mersa Matruh to the coast of Lebanon.

The Rhodes gyre is not as intense in winter as in the summer and also appears to weaken with depth. However, it covers an extensive crescent-shaped area surrounding the anticyclonic Mersa Matruh gyre to its south. On both sides of the Mersa Matruh gyre, the lateral extensions of the Rhodes gyre almost abut the southern coast of the Basin.

As before the waters within the Cilician basin are divided into a number of cyclonic and anticyclonic eddies, giving the impression of a meandering Cilician current in the lee of Cyprus.

At intermediate depths, the eddies in the Antalya Gulf and to the south of Cyprus intensify. At 600 db, the main eddies that remain identifiable are the anticyclonic Mersa Matruh and Shikmona gyres. The zonal flow at 34°30'N in the west is probably an artefact resulting from data mismatches between the two parts of the survey; it only becomes noticeable when the true anomaly fields become small at these deeper depths.

Yet again Ovchinnikov and collaborators (Ovchinnikov *et al.*, 1976) appear to have reached entirely different conclusions. Their winter maps (at the surface, 100, 250 and 500m) show the

(a)

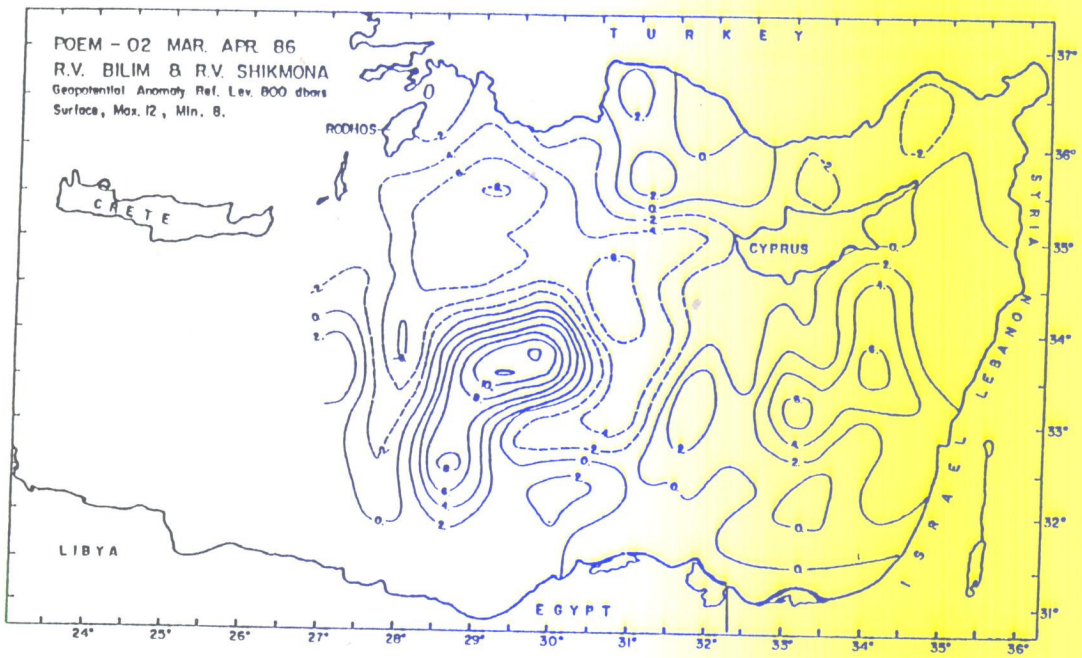

(b)

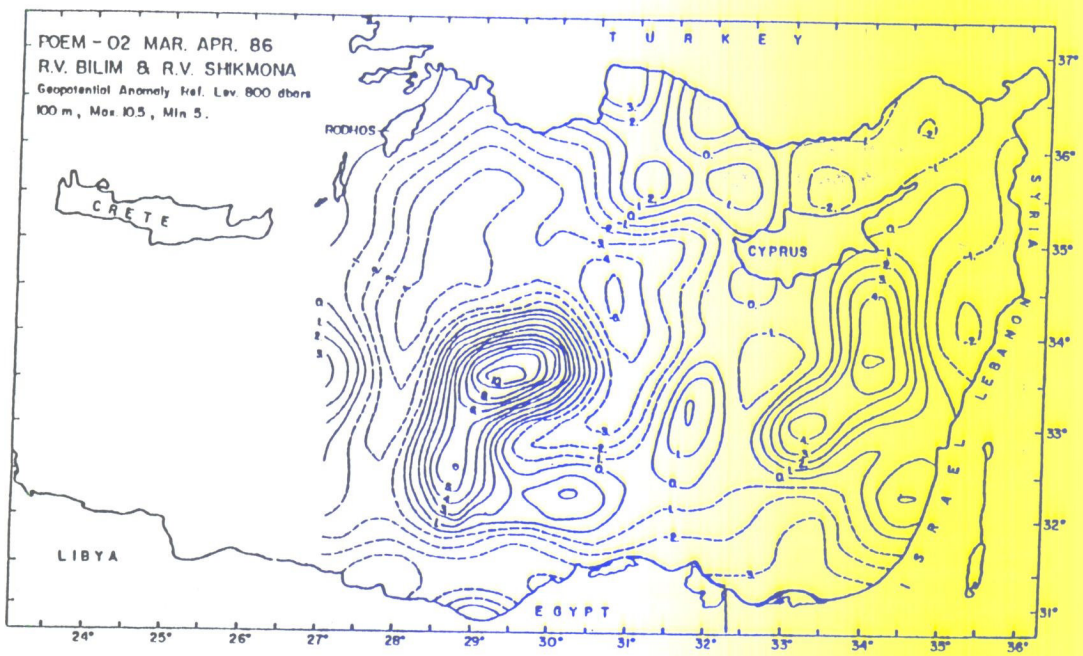

FIG. 4. Objective analysis of the geopotential anomaly of (a) the surface, (b) 100, (c) 200, (d) 300 and (3) 600 dbar surfaces (relative to 800dbar) based on the combined MA86 data. (See Fig.3).

(c)

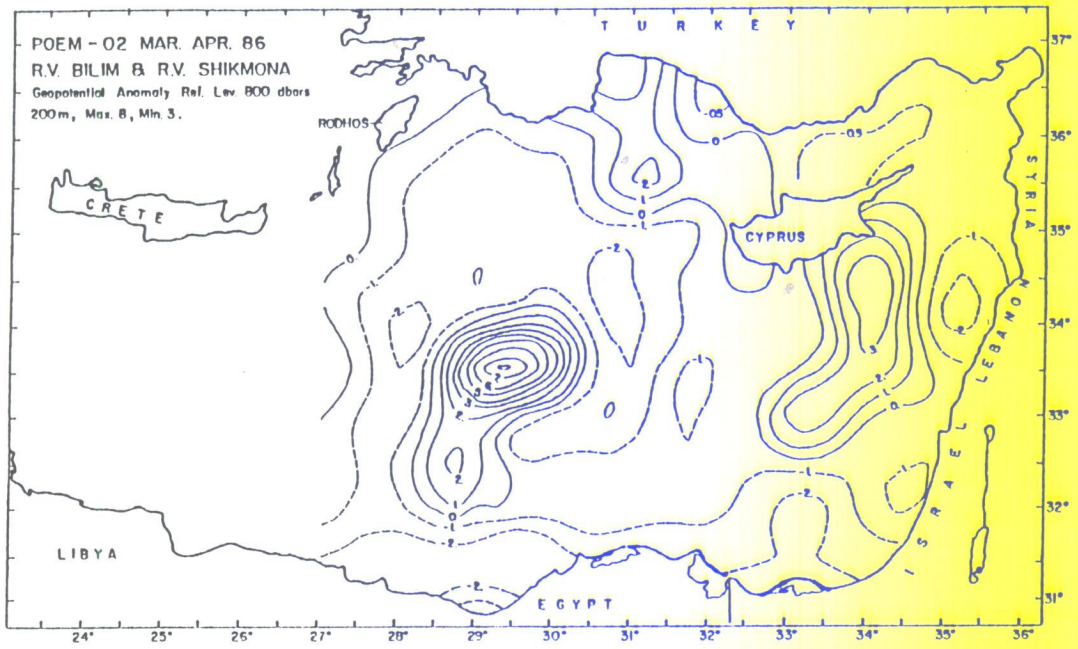

(d)

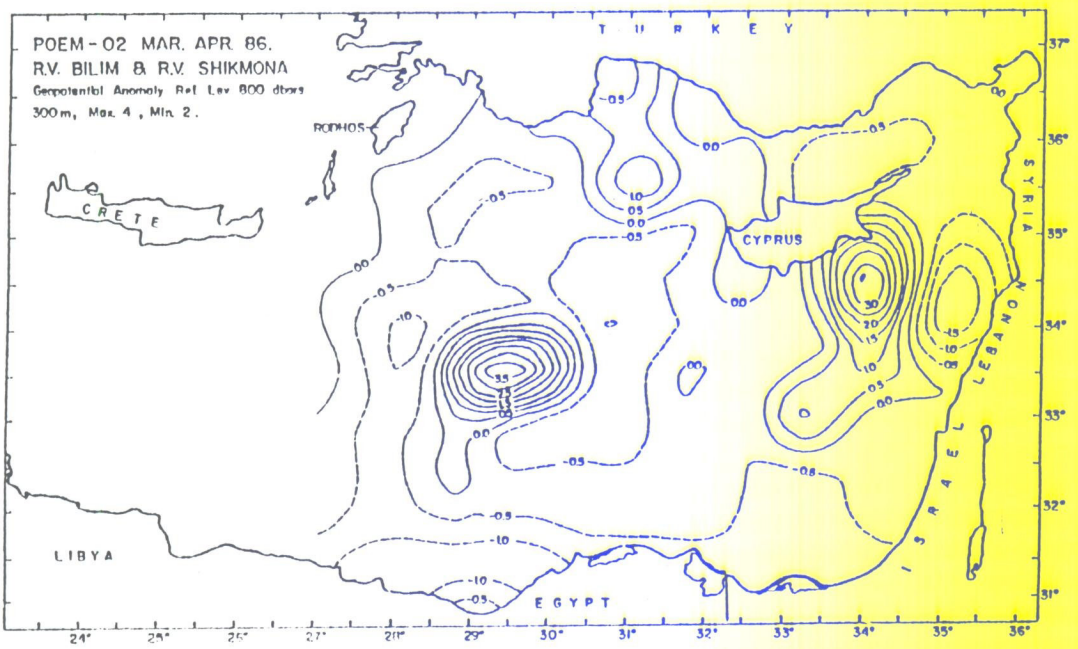

FIG. 4. Continued.

(e)

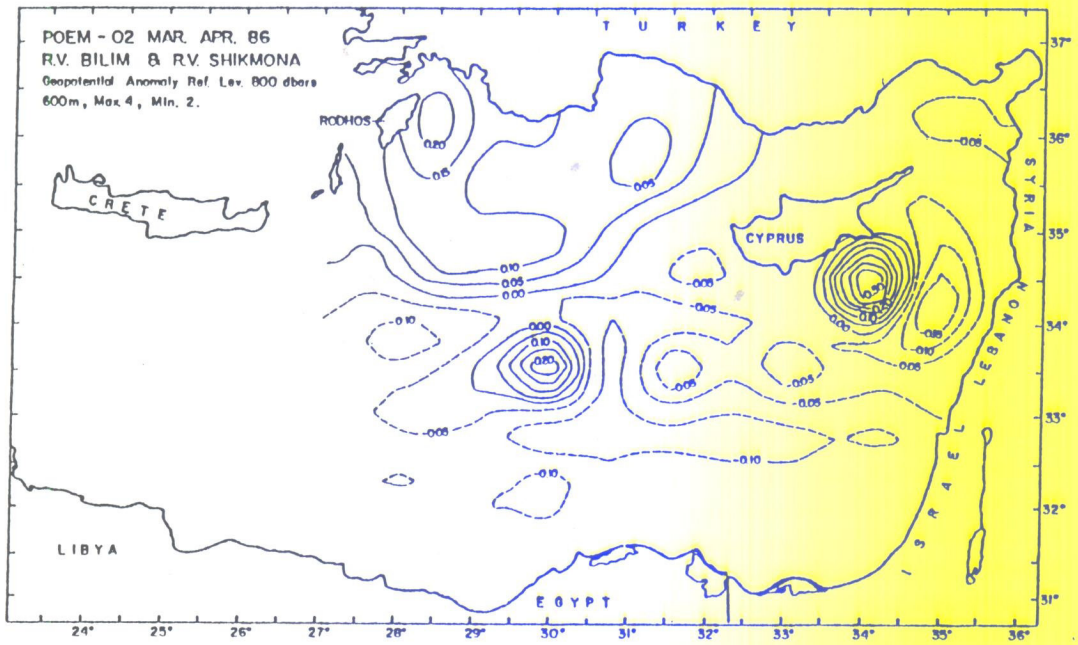

Fig. 4. Continued.

CLBC entering the Basin through the southern part of the Cretan Passage, flowing as far as the coast of Israel where it turns northward, runs around Cyprus, then westward through the Cilician Basin and into the Ionian Sea through the northern section of the Cretan Passage. That is to say, a general cyclonic pattern similar to their description of the summer circulation. West of Cyprus, this stream appears to branch off northward, forming a large cyclonic gyre in the central and northern Levantine Basin (the Rhodes gyre?) and southeast of Cyprus, another branch forms another cyclonic eddy close to the Israeli coast.

In general, finer scale features are more dominant in winter than in summer, because of the reduced stability (i.e. smaller radius of deformation) in winter. The sharpest gradients occur at the periphery of the Mersa Matruh gyre (where current velocities of at least 35 cm s^{-1} are found and remembering the station spacing and the smoothing effect of objective analysis, observations at any point around the periphery may give much higher velocities). The major gyres are not homogeneous in their interior regions because of the smaller scale of the variability. For example, the Rhodes gyre fragments into smaller cells approximately near 35°N 30°E and also near 34°30′ N 28°E. Similarly, the Mersa Matruh gyre has secondary centres located at 32° 30′N 28° 30′ E and 32°N 30°E.

It is important to note that the Rhodes and the Mersa Matruh gyres appear to be paired together in both cruises. In both surveys, the importance of baroclinic components in the circulation is emphasized by both the significant vertical structure displayed in the estimates, and the density structure imposed by the interspersed water masses (see Section 5). Potential energy is available to maintain such activity, as will be reported for the present surveys in another publication.

An important feature inferred from the above is the separation of anticyclonic eddies into smaller multiple centres of varying intensity with increasing depth. Such multiple cells merging into a single anticyclonic eddy near the surface are observed in the Gulf of Antalya, the southwestern and the southeastern regions of the Basin during both surveys. The structure of

these eddies is strongly reminiscent of nonlinear eddy mergers investigated by Nof and Simon (1987). The merging of eddies in the Levantine Basin is to be expected in view of the small size of the basin and the horizontal extent of the eddies, which should bring them into frequent contact.

It is also important to recognize the similarities in circulation between the two surveys reported, in spite of the fact that they are separated in time by several months. The main features appear to be persistent, although modified in form. It seems likely that the main gyres are quasi-permanent, although they may display seasonal and interannual variability. Furthermore, some of the mesoscale eddies have been shown to persist for about a year in the southeastern Levantine Basin by Feliks and Itzikowitz (1987) and Hecht, Pinardi and Robinson (1988).

6. HYDROGRAPHY

6.1. *ON85*

The most distinctive hydrographic characteristic of the Levantine Basin is its extreme variability, which we initially illustrate with profiles obtained at selected stations. In ON85 (Fig.5) the LIW (characterized by warm saline waters) is found at station 242, located at the centre of the Antalya anticyclonic eddy down to a depth of 400db and with a maximum salinity of about 39.1. At the same station, the occurrence of AW is shown in the trace below the mixed layer. In contrast the profile for station 237 located at the centre of the Rhodes gyre shows almost uniform properties, with a surface layer almost indistinguishable from the underlying cold, low salinity waters, characterizing the upwelling Rhodes dome. The profile from station 353 within the Mersa Matruh gyre shows AW occupying a depth of 300db with a minimum salinity of 38.5 below a relatively thick mixed layer. Immediately northeast of this gyre at station 329, a 100db thick layer of AW is still found, but high salinity waters of about 39.0 appear between the 150-500db levels. This latter station was located in the northeasterly gyre of the deep twin anticyclonic features observed in the region.

The variations in the Θ-S relationships that occur between clusters of stations A, B and C,

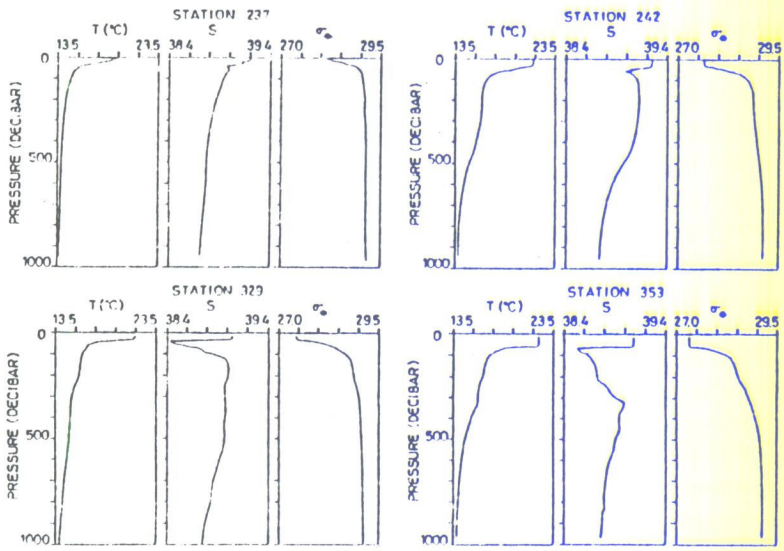

Fig.5. Selected profiles of temperature, salinity and density (σ_θ), ON85 cruise.

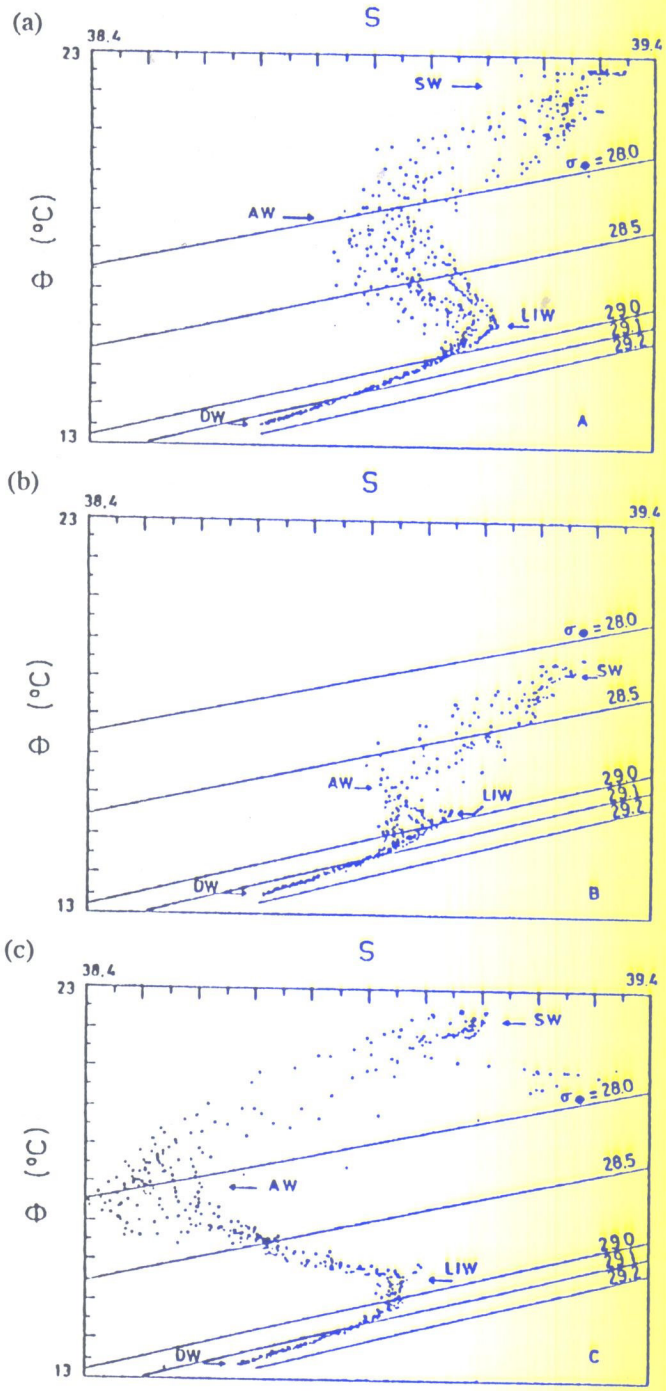

FIG.6. Potential temperature (Θ) and salinity (S) relationships for clusters of stations in areas (a) A, (b) B and (c) C marked in Fig.2a, ON85.

marked in Fig.2a and corresponding respectively to the Antalya, Rhodes and Mersa Matruh eddies, are illustrated in Figs 6a, b and c. The surface waters (SW), the layer marked by the AW influence, the LIW, and the transition to deep waters are identified in the Figures. In clusters A and C, warm saline waters near the top characterize the surface layer. The maximum AW signature occurs in area C, and some of its influence penetrates into area A immediately below the surface layer. In comparison, the Rhodes gyre waters (area B) approach towards more homogeneous characteristics: The surface waters are colder than the other areas by an average 3°C, and both the AW and the LIW anomalies occur in smaller and thinner layers that appear closer to the surface (see also station 237, Fig.5). The LIW core has its highest salinity and temperature in area A, with maximum values of 39.12 and 16.1°C respectively.

The water mass distribution characteristics are now shown along selected vertical sections. The contour intervals in the salinity sections have been stretched so as to facilitate their interpretation assuming that the dashed lines (salinity of 38.95) indicate the lower limits of LIW, and the salinities <39.0 (solid lines) immediately below the mixed layer and above the LIW indicate AW masses. The sections have been plotted only to depths of 400db so that the details in the upper layers are enhanced. The deeper structure is similar but weaker, although in some of the anticyclonic eddies the temperature-salinity signatures may extend to depths of 1000db.

Along the northernmost east-west transect, the vertically-uniform mixed layer shows significant horizontal variations (Fig.7a) in temperature and in its depth; the regions where the mixed layer is deeper coincide with anticyclonic convergence zones, and regions of the shallower mixed layer occur in cyclonic zones. At the station 205, the cold dome of the Rhodes gyre can be seen; two anticyclonic eddies are located respectively at stations 203 and 200. A series of shallow eddies are indicated in the Cilician Basin. In the salinity section (Fig.7b), high salinities appear in the mixed layer, below which narrow filaments of AW with varying salinity minima are observed. Deeper down, a nearly homogeneous mass of LIW is found between depths of 100-400db. The only location where this structure is disrupted completely is at the Rhodes cold dome to the west, where neither AW nor LIW can be differentiated clearly.

Figure 8 displays a salinity section to the west of Cyprus. It shows AW circulating around the easterly extension of the Rhodes gyre and intruding into the northern Levantine Basin in the form of filaments below the mixed layer. Further north these waters appear as much diffused patches which are continuations of the filaments. The salinity contours are generally shallower than in the section shown in Fig.7b, because of the easterly extension of the Rhodes gyre.

Figures 9a and b show the east-west temperature and salinity transects along 34° N. Cold water is doming at the cyclonic centres to the southwest and southeast of Crete. Between these centres are small scale anticyclonic eddies where LIW with high salinities occurs at the surface and extends downwards sinking to a depth of 300db. These features are arranged along the southwestern edge of the Rhodes gyre. The strong jet flow separating the Rhodes and the Mersa Matruh-Shikmona gyre complex (i.e. the CLBC) is shown to have trapped a large quantity of AW in the upper layers, extending towards southern Cyprus. The AW displays several temperature and salinity inversions that are characteristic of intrusive layering at this frontal region. A separate filament of AW is found in the northeasterly jet flow south of Crete, indicating advection by the postulated southwest Cretan eddy. In the eastern region of the Levantine Basin, LIW is found at greater depths underlying the AW, and it increases in abundance towards the eastern coast, where it is again trapped in an anticyclonic eddy that preserves its intensity with depth.

The salinity section along 33°30′N is illustrated in Fig. 10. South of Crete, it differs markedly from the section along 34°N shown in Fig. 9b. There is an abundance of low salinity AW in the southern part of the Cretan Passage. The patch of LIW observed along 34°N is much reduced

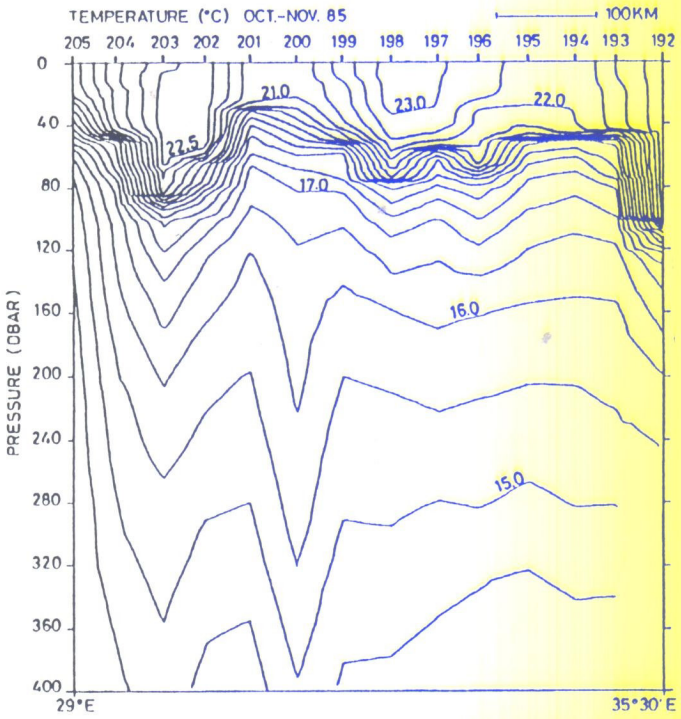

Fig.7a. Temperature east-west section along 36°N, for the ON85 survey. A 0.5°C temperature contour interval has been used in all ON85 sections.

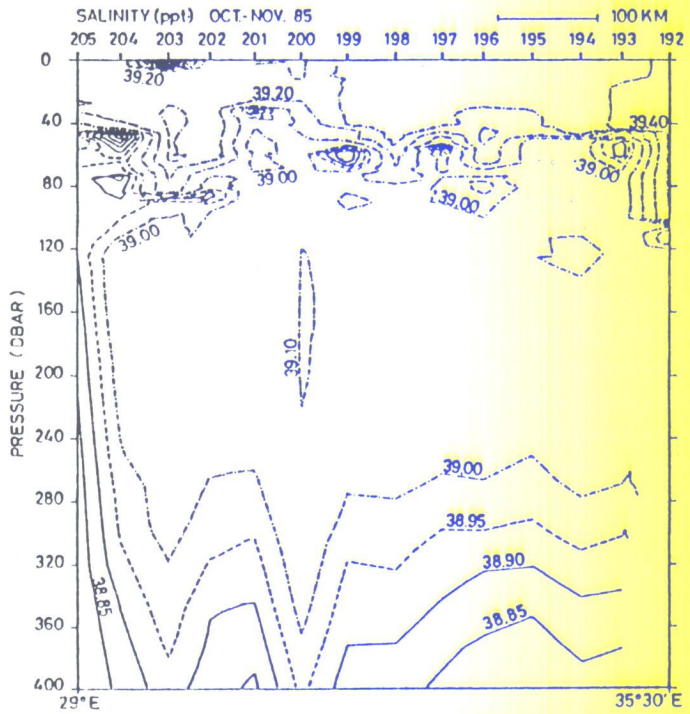

Fig.7b. Salinity east-west section along 36°N, for the ON85 survey. Variable salinity contour intervals of 0.05 for salinities <39.0 (solid lines up to 38.9 and a single dashed line for the 38.95 contour) and 0.1 for salinities >39.0 (dot-dashed lines) have been used in all ON85 sections.

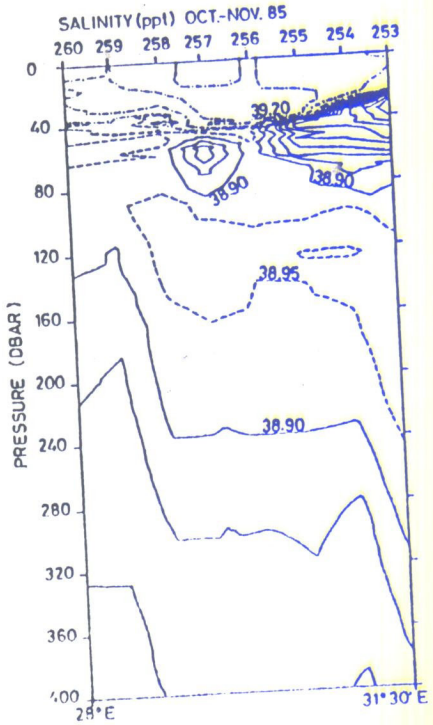

Fig.8. Salinity east-west section along 35°N, west of Cyprus, ON85.

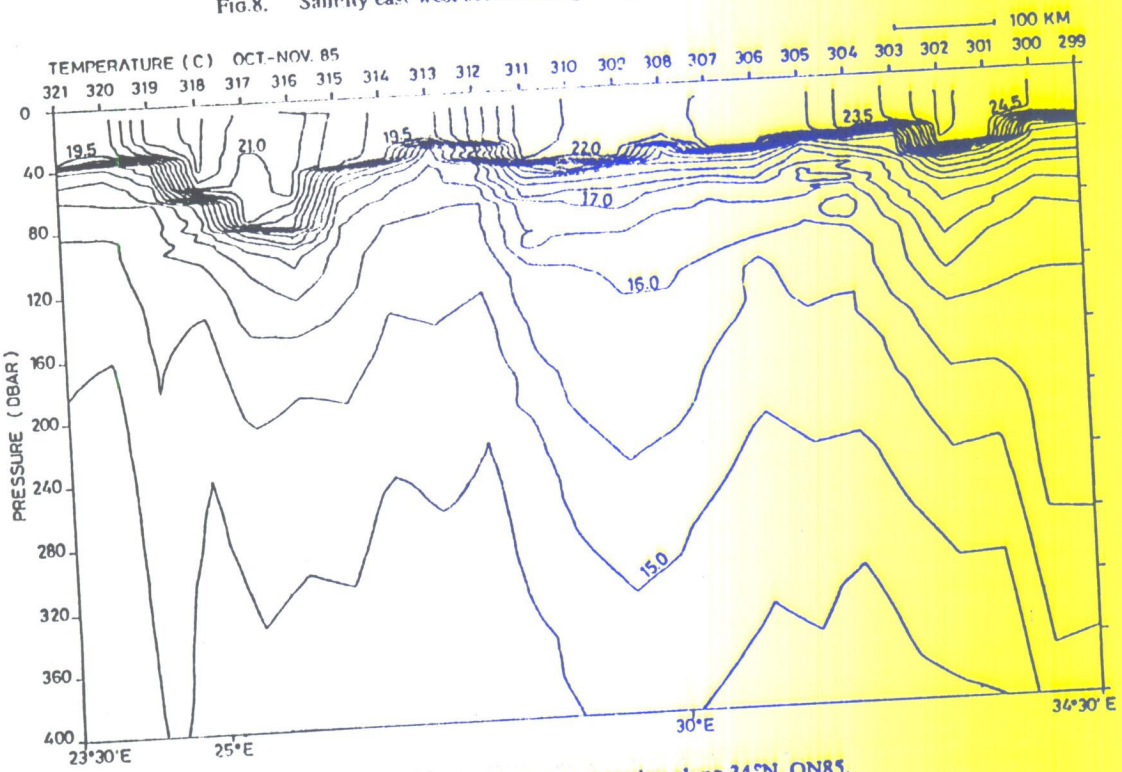

Fig.9a. Temperature east-west section along 34°N, ON85.

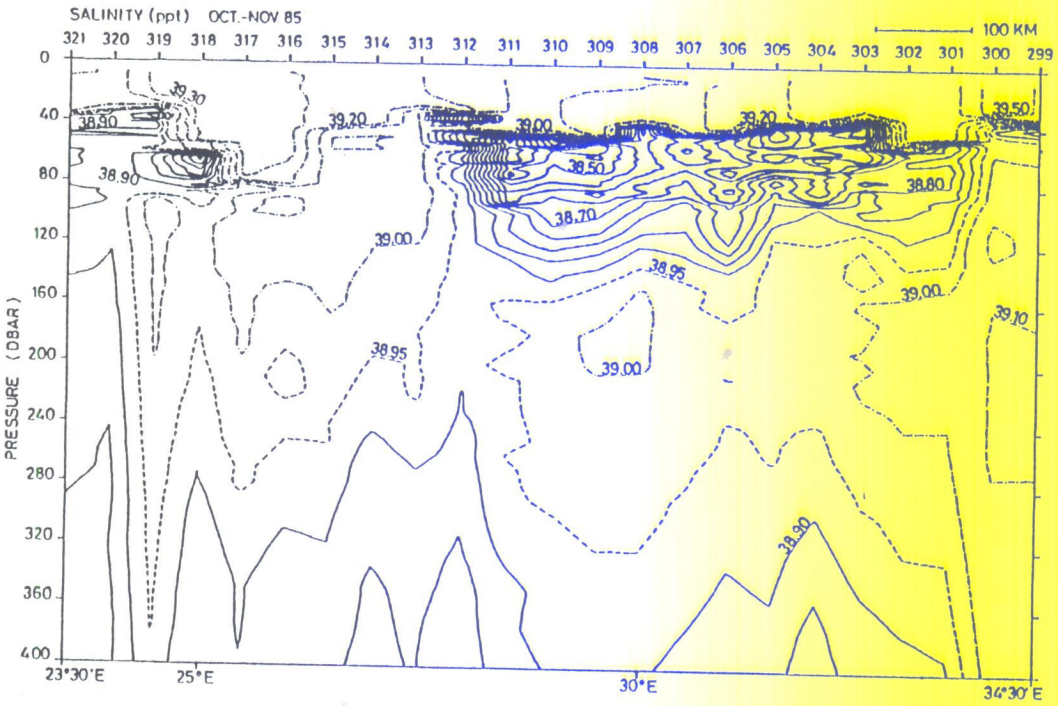

Fig.9b . Salinity east-west section along 34°N, ON85.

in size because this section is generally offset from the periphery of the Rhodes gyre, along which the sinking process appears to be confined. Likewise, AW is only briefly intercepted at station 325 which was located on the edge of the Rhodes gyre. In the eastern part of the section, both AW and LIW are found in their respective layers. The core of the deep anticyclonic eddy at station 329 traps LIW at deeper layers

In the next section to the south along 33°N shown in Fig. 11, large volumes of AW are displayed entrapped in the Mersa Matruh and Shikmona anticyclonic circulations. The maximum quantities of LIW are found in the southeast within the Shikmona gyre region, although it also appears below the AW pooled in the Mersa Matruh gyre down to 40db.

This description of hydrographic variability is supported by selected north-south sections of salinity along 34°30′E, 31°30′E, 29°30′E and 28°30′E in Figs 12a-d respectively. Along 34°30′E, LIW is most abundant all along the eastern coast and its entrapment in the deep Shikmona gyre can be inferred. In the other sections, LIW is again observed to be concentrated in anticyclonic eddies occurring on both sides of the extension of the Rhodes gyre. In the northern parts, where the AW intrusion is minimal, the high salinity water extends to the surface, while it may underlie AW in the southern eddies. The westernmost section shows LIW trapped between the Rhodes gyre and the Rhodes-Anatolian coasts

6.2. *MA86*

In the profiles selected from the MA86 set of observations (Fig. 13), the subsurface waters were mixed down to depths of 200-400db. Only at very few stations in the northern region of the Levantine Basin were occasional traces of AW found, such as at station 885. At certain locations near the northern coast, the LIW was found down to depths of 400db, as shown in the profile for

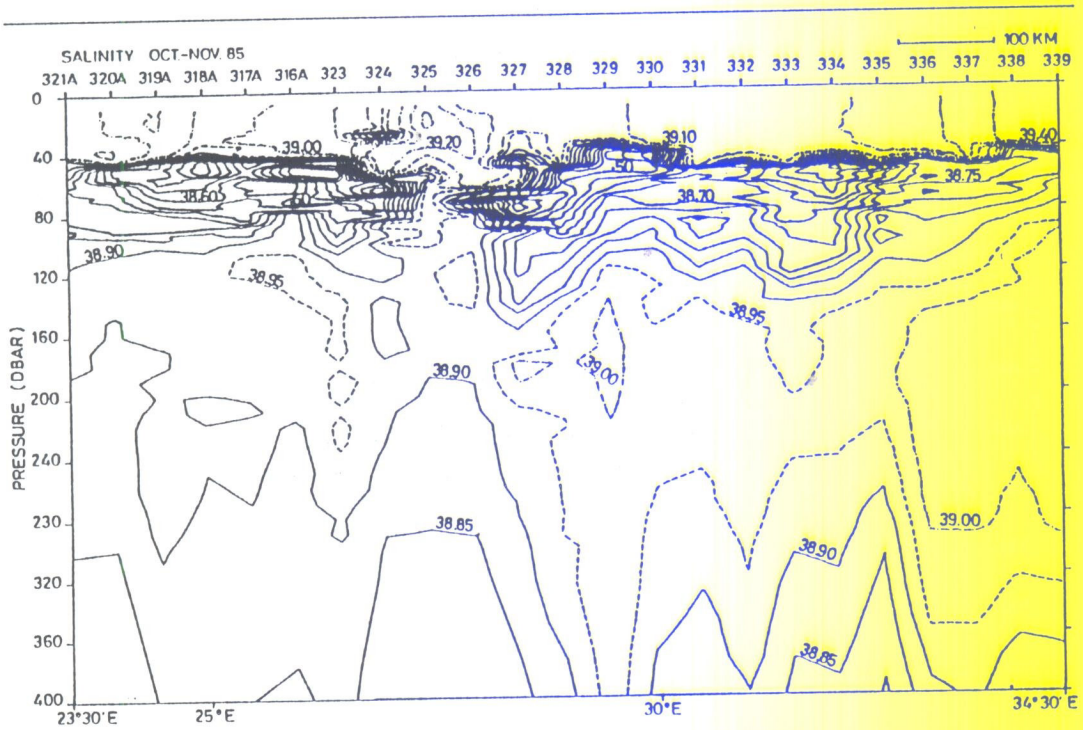

Fig.10. Salinity east-west section along 33°30'N, ON85.

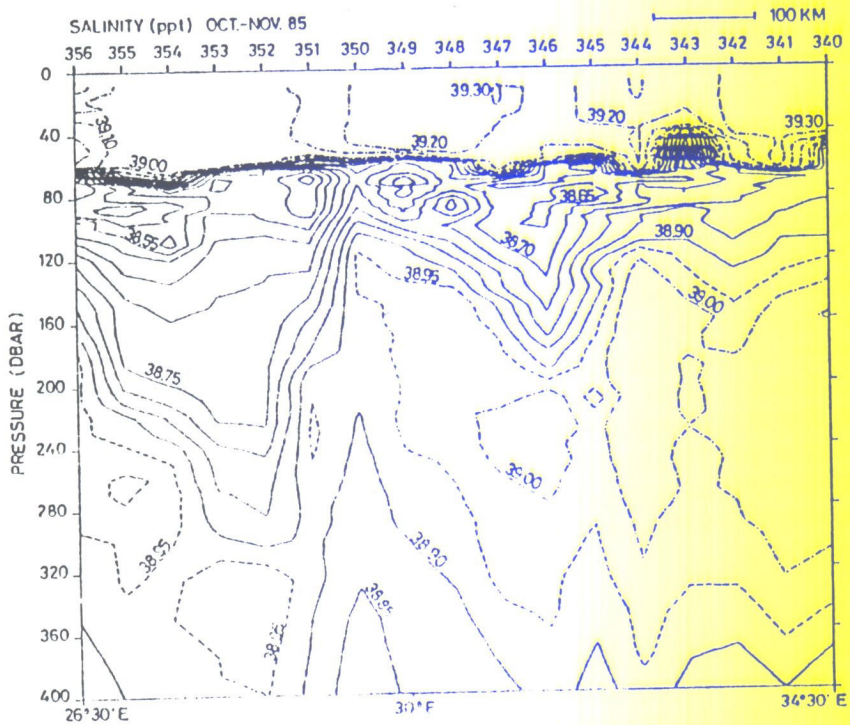

Fig.11. Salinity east-west section along 33°N, ON85.

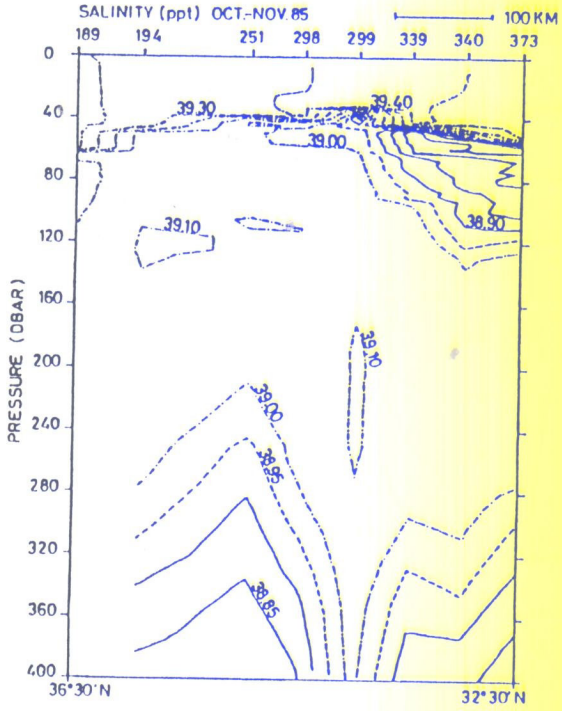

FIG. 12a. Salinity north-south section along 34°30 E, ON85.

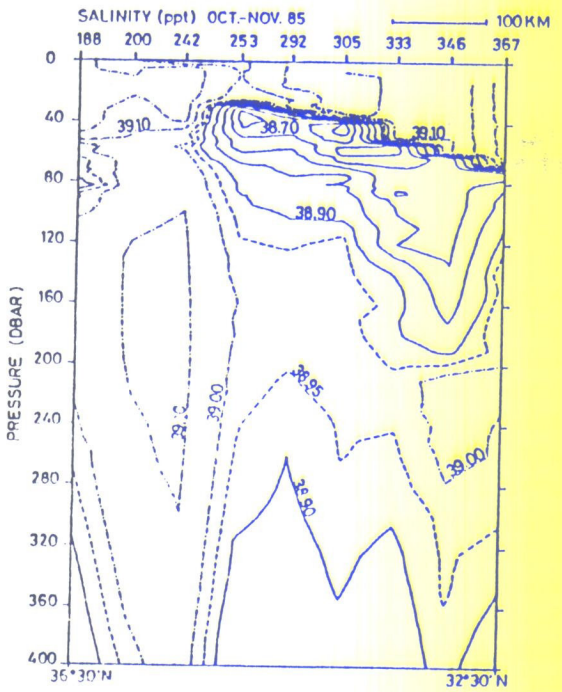

FIG. 12b. Salinity north-south section along 31°30 E, ON85.

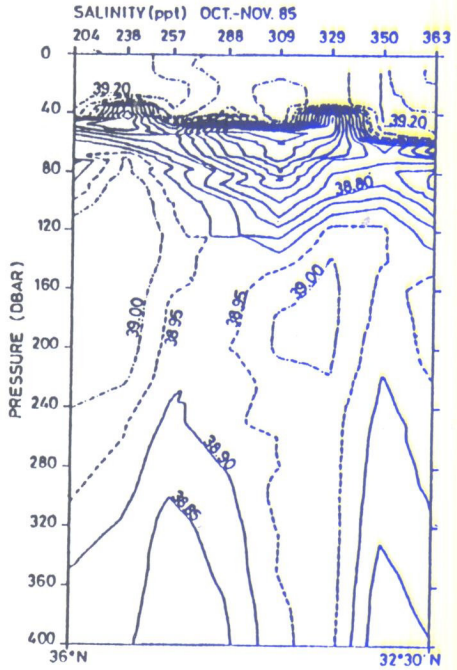

Fig.12c. Salinity north-south section along 29°30'E, ON85.

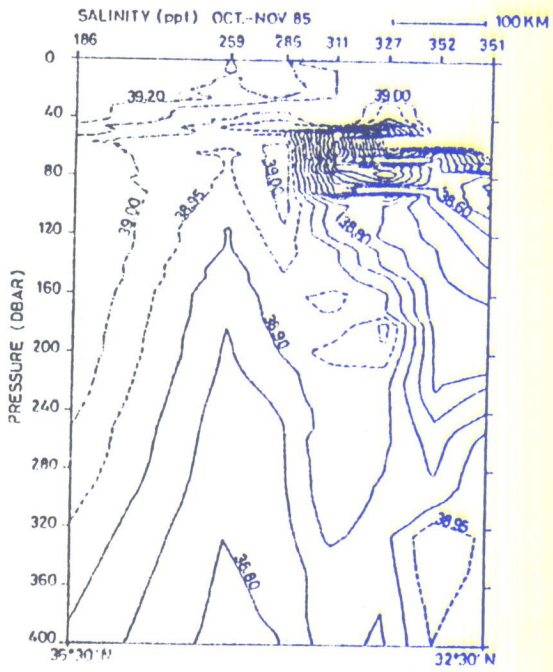

Fig.12d. Salinity north-south section along 28°30'E, ON85.

station 95 in the Gulf of Antalya. The trapping of AW in the Mersa Matruh gyre is seen in the profiles from stations 308 and 361, where the low salinity surface waters reach a depth of 300db. Note the surface mixed layer had not started to form, so that the AW occurred at the surface. Intrusive layering of the water type observed at station 308 also occurred at other stations in the vicinity of filaments and fronts in the region.

Smaller scale details are exhibited in the winter, as a consequence of the reduction in the

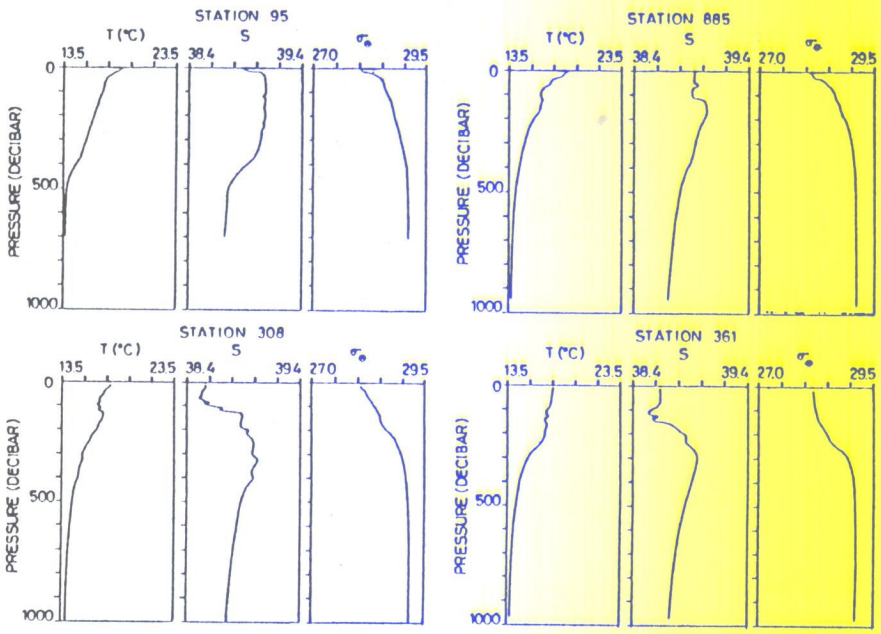

FIG.13. Selected profiles of temperature, salinity and density (σ_θ), MA86 cruise.

intensity of stratification and the increased mixing of the upper levels. The high salinity waters generally extend from the surface to intermediate depths with relatively more uniform properties, and the identifiable intrusions of AW are more restricted because of the increased mixing.

The Θ-S diagrams for station clusters in areas A, B and C (see Fig.2b) are presented in Figs 14a, b and c respectively. In area A, the surface and intermediate waters are almost uniform in salinity, although the temperature stratification extends throughout the surface and AW layers (see also the profiles for station 95, Fig.13). Part of the variation in temperature is caused by early spring warming of the near surface waters, confined in the upper 25-50m, and partly by the small patches of AW intrusions (see adjoining station 885, Fig.13). In any case, these effects are limited to the upper 100m and in most of the profiles LIW approaches closer to the surface. The LIW in this region preserves the maximum salinity and temperature values found in summer in the same area (compared with cluster A, Fig.6). In area B, the water column becomes less stratified, with the surface effects being confined to a very thin layer, as a result of which the surface waters reach the highest densities of all regions. On the other hand, the AW has a significant influence in area C, where it starts from the surface and overlies the other water masses as a relatively thick layer.

We further describe the water mass distribution on vertical sections. Along 36°N the salinity

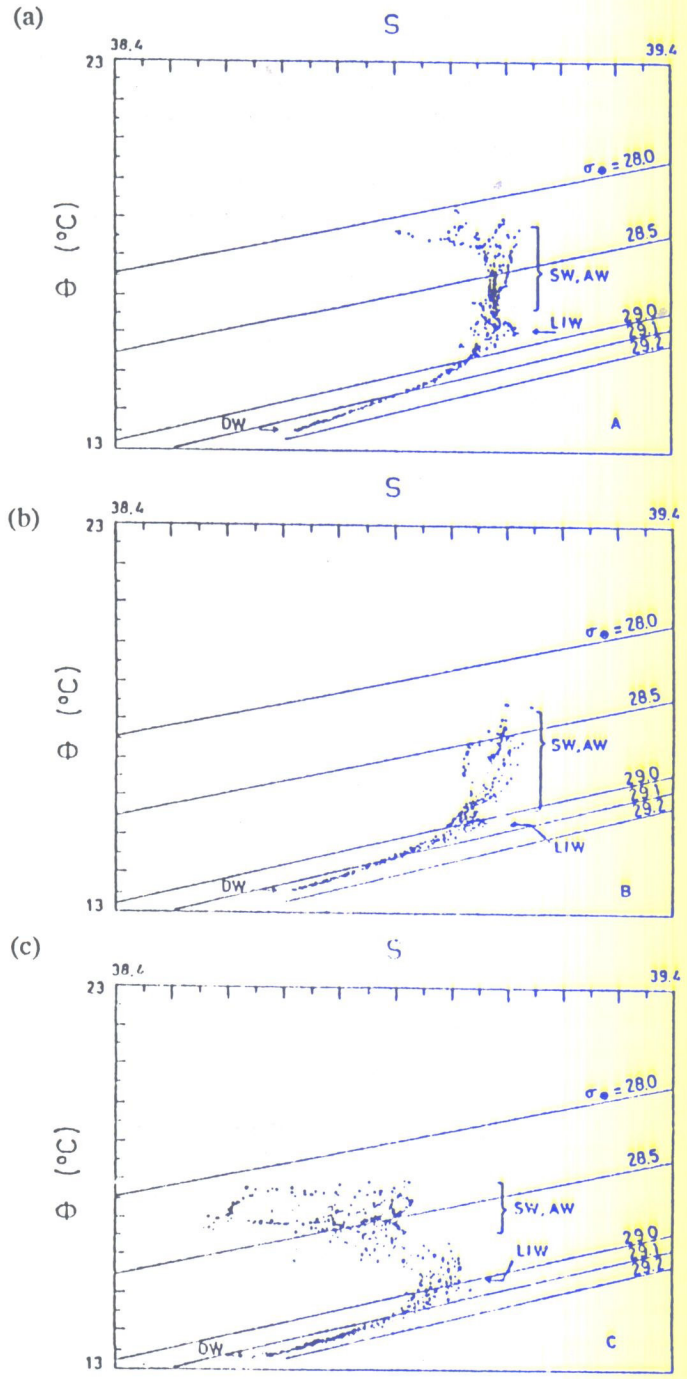

FIG. 14. Potential temperature (Θ) and salinity (S) relationships for clusters of stations in areas (a) A, (b) B, and (c) C marked in Fig. 2b, MA86.

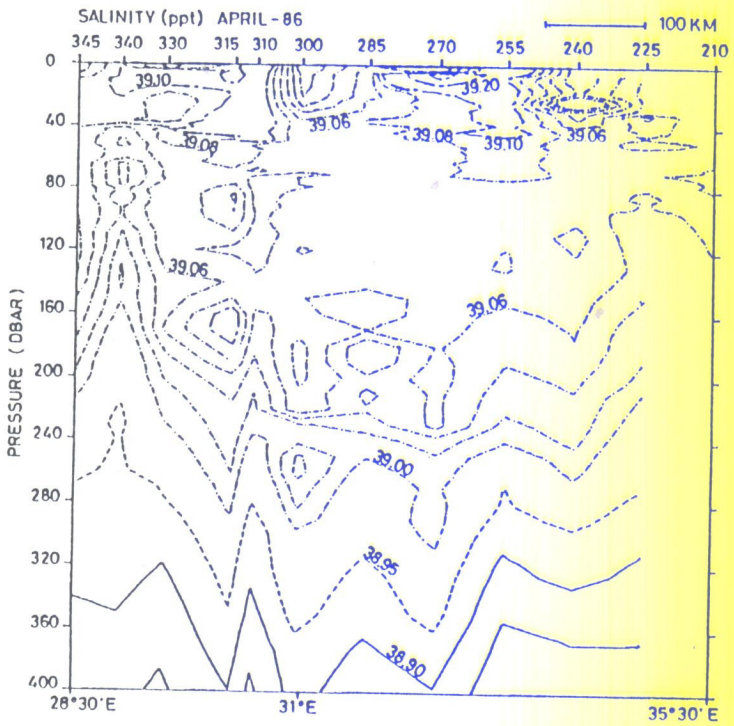

FIG.15. Salinity east-west section along 36°N, MA86. Variable contour intervals of 0.05 for salinity values <39.0 (solid lines up to 38.9 and a single dashed line for the 38.95 contour) 0.02.

section (Fig.15) indicates that high salinity waters extended from the surface down to depths of 300db. At station 340, part of the Rhodes upwelling dome is observed, but the Rhodes dome is more clearly seen along the eastern sector of the 35°30′ N sections (temperature and salinity) displayed in Figs 16a and b. A maximum in LIW is observed at depths of 200-300db within the Gulf of Antalya anticyclonic eddy immediately adjoining the cold dome.

As discussed in Section 5, the Rhodes gyre is in a nonuniform crescentic form encircling an anticyclonic gyre. In Fig. 17 which is the salinity section along 35°N a small scale LIW sinking patch is displayed at station 730 which was located in one of the narrow sections of the Rhodes gyre arm, where the anticyclonic eddies lying on either side are tending to converge.

The sections along 34°N (Figs 18a,b) display upward injections of the underlying water in the narrow west arm of the crescent shaped Rhodes cyclonic circulation. A mass of AW at the surface occupies the west side of this section and is entrapped within the Mersa Matruh gyre. There is a sharp front separating this gyre from the east arm of the Rhodes gyre. The LIW is entrapped at deeper layers within the Mersa Matruh gyre and also occurs in the eastern Levantine Basin where it is found immediately below the surface. A maximum in LIW occurs at station 300 within an anticyclonic cell of the Shikmona gyre. Some traces of AW appear at the surface.

Along 33°30′N (Figs 19a,b), the situation is similar except that the vertical motions are more intense. The AW entrapped in the Mersa Matruh gyre appears in two separate patches with extensive vertical elongations. The salinity section further south along 33°N (Fig.20) shows a narrower cell representing the southern extremity of the Mersa Matruh anticyclone and increased

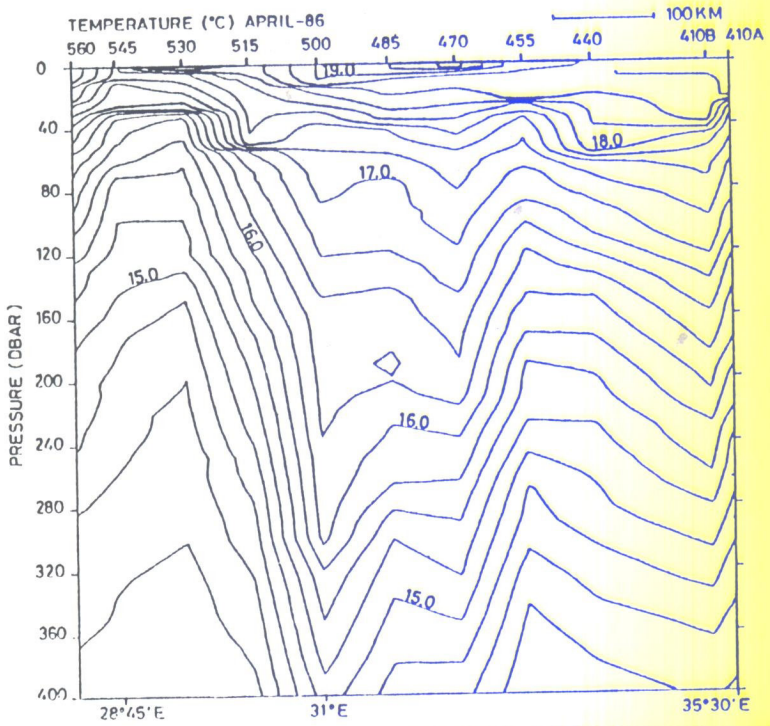

Fig.16a. Temperature east-west sections along 35° 30'N, MA86. A 0.25°C temperature contour interval has been used in all MA86 sections.

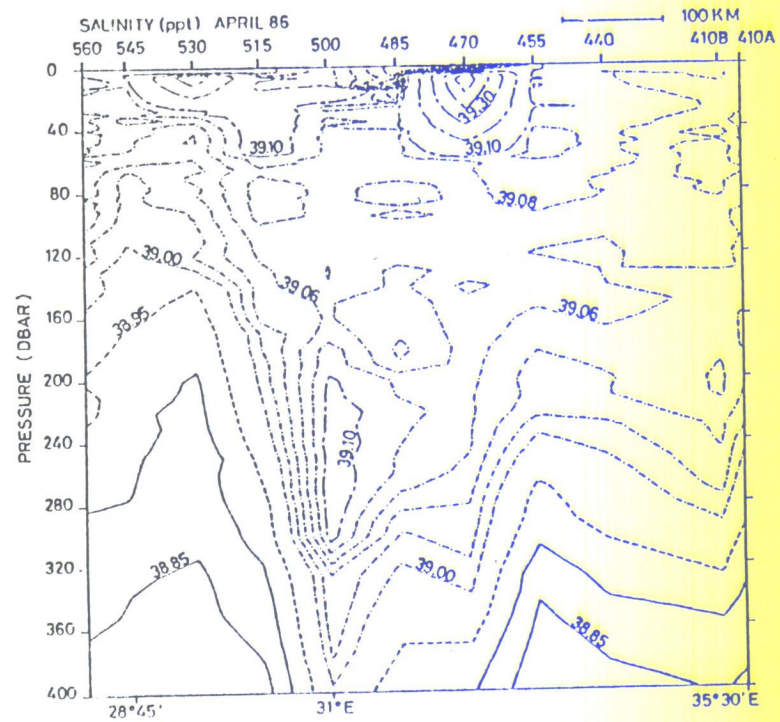

Fig.16b. Salinity east-west section along 35°30'N, MA86.

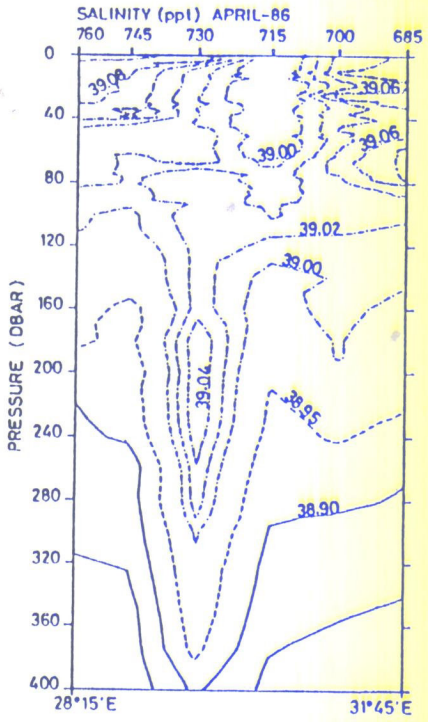

Fig.17. Salinity east-west section along 35°N, MA86.

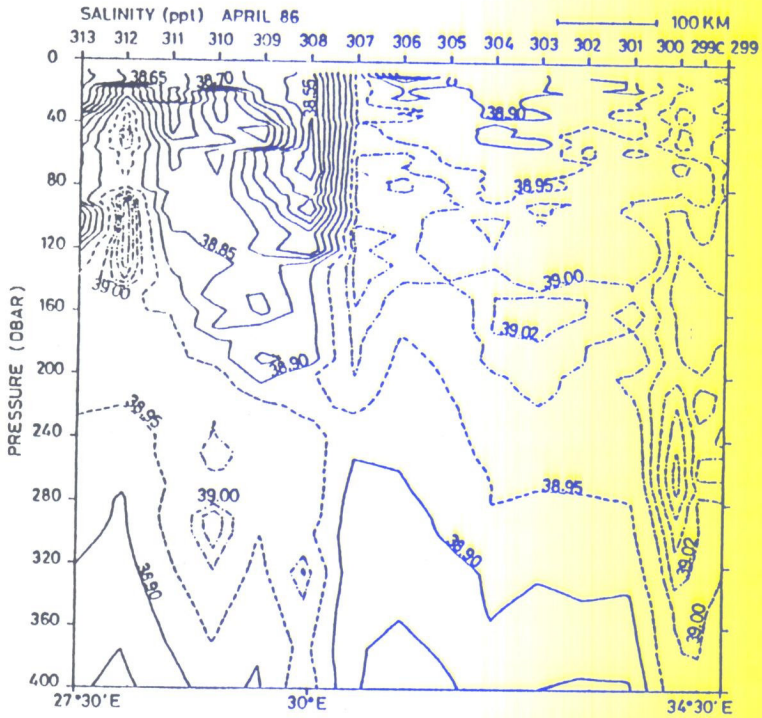

Fig.18a. Temperature east-west section along 34°N, MA86.

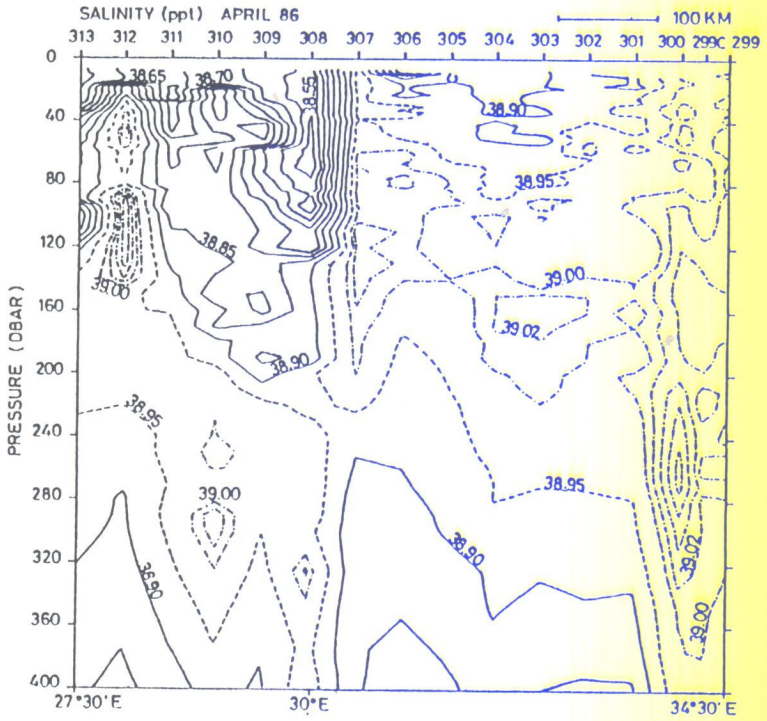

Fig.18b. Salinity east-west section along 34°N, MA86.

penetration of the near-surface AW towards the east. The LIW is observed near the southern periphery of the Rhodes gyre east arm and is also entrapped in the anticyclonic eddies in the Shikmona gyre region.

The north-south salinity section in the west of the survey area (Fig.21) indicates that to the northwest of the Rhodes gyre, LIW is abundant, becomes shallower over the Rhodes dome and is then bounded by the sharp front which separates it from the AW pool to the south.

7. BULK HEAT STORAGE, AW AND LIW VOLUMES

The hydrography of the Levantine Basin is shown to have a complex structure. The various water masses at different depths are advected by and trapped within the general and eddy circulations, continually evolving in character through mixing processes and surface fluxes. Consequently no single water mass can at any one time be identified by a tight envelope of T-S characteristics. In this respect, volumetric T-S analysis can only yield the regional distribution of the statistics associated with the permanent water masses. Utilized as such, the volumetric T-S analysis (e.g. Miller, Tchernia, Charnock and McGill, 1970) could not easily be related to the meso-scale processes emphasized in the earlier sections.

An alternative to T-S analysis is therefore volumetric computations displaying regional differences in the abundance of the various water masses. For this purpose, the vertical profiles were integrated between logically pre-selected intervals, to determine heat and salt content per unit surface area.

The heat content is computed from the product of the temperature excess with respect to 15°C with the corresponding specific heat. The integration is carried out to a depth of 250db to characterize the near-surface properties. The results are given in units of kcal cm^{-2} .

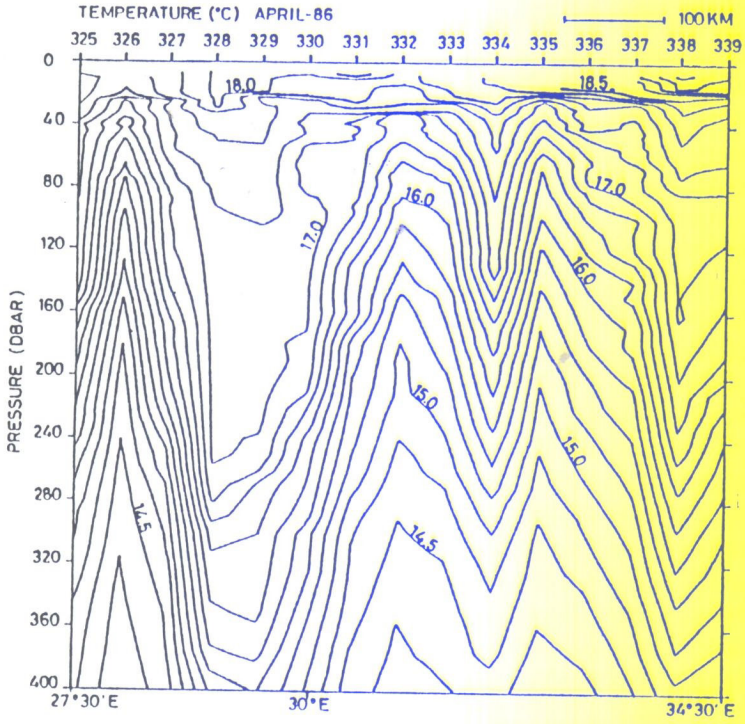

Fig. 19a. Temperature east-west section along 33°30'N, MA86.

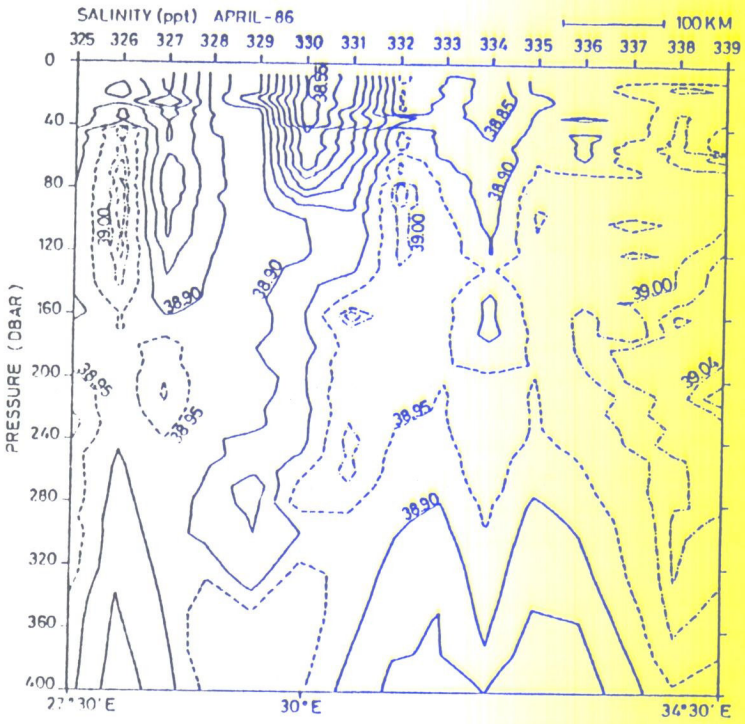

Fig. 19b. Salinity east-west section along 33°30'N, MA86.

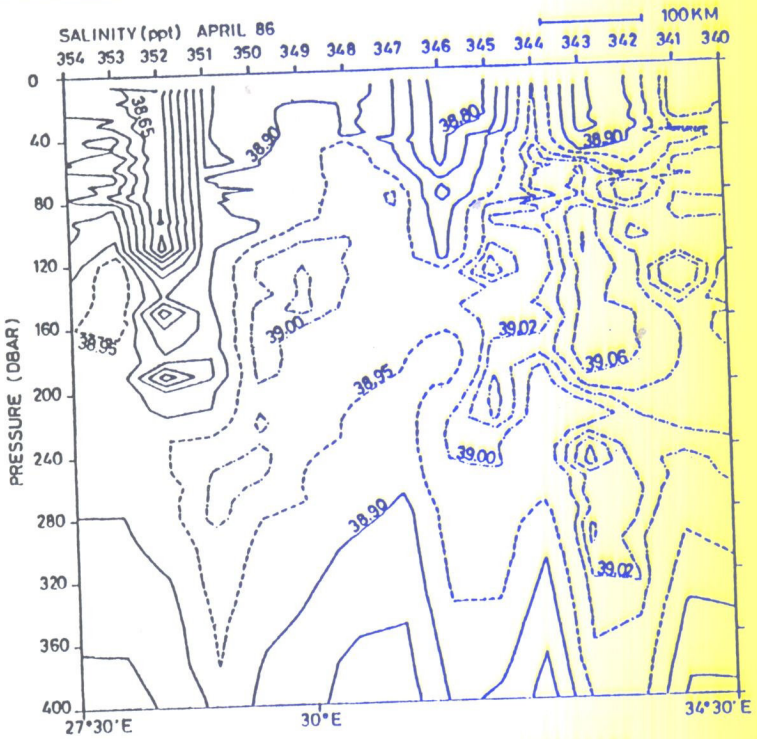

Fig.20. Salinity east-west section along 33°N, MA86.

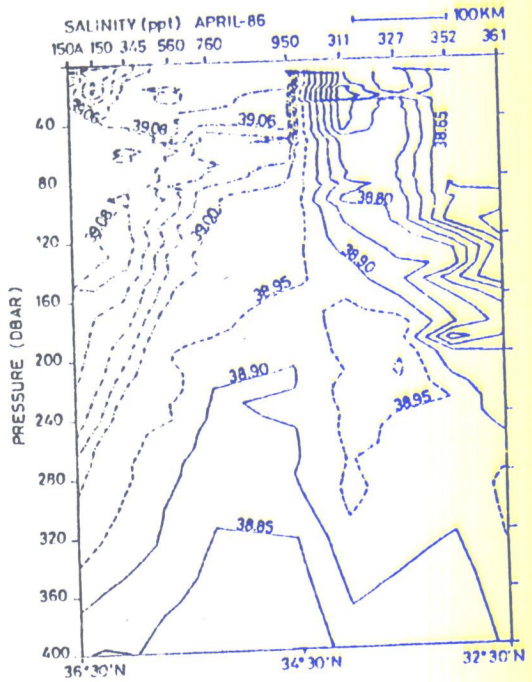

Fig.21. Salinity north-south section along 28°30'N (approximate longitude), MA86.

The computation of salt content within a prescribed depth is not suited for the Levantine Basin, since the mixing ratio of the typical water masses is variable at each station. The salt content of each water type has to be determined separately in order to distinguish their relative influences. Since the salinity cutoff values assigned for defining each type of water varies from one station to another, these limits are essentially selected after a review of the data. The salinity upper limits used in the integration for identifying the AW have been chosen slightly above the maximum value observed in the survey domain of the AW salinity minimum. This yielded a salinity upper limit of 39.1 for AW in the ON85 survey. Since the vertical distribution was more uniform in the MA86 survey, a salinity upper limit of 39.0 was utilized. The salinity difference with respect to these limits was then integrated with respect to depth, by multiplying it with density to yield AW salt anomaly in units of kg m^{-2} . The integration was performed starting below the mixed layer in the summer survey, and from the surface in the winter survey, down to either the depth of intersection with the cutoff value, or the depth of the intermediate salinity maximum where an intersection did not occur. Similarly, the lower salinity limits selected for LIW are slightly lower than the minimum value observed over the domain of the LIW salinity maximum; a salinity lower limit of 38.9 was used in the analysis of both surveys. The integration of the positive salt anomaly was carried out for the zone with salinity in excess of the assigned lower limit, starting from below the AW signature (AW salinity minimum, if present) and extending down to the depth at which the deep water salinity became <38.9. In both procedures, logical checks were applied to determine overlaps of the depth ranges and to exclude data increments not conforming to the salinity limits. The heat storage, and negative and positive salt anomalies, corresponding to AW and LIW respectively, are presented in the following.

7.1. *ON85*

The 250db, 15°C referenced heat content in Fig. 22a shows that the minimum heat storage occurred in the Rhodes gyre and its extension, and partially to the east of Cyprus. The maximum of heat storage occurred in anticyclonic eddies observed near Rhodes, in the Gulf of Antalya-Cilician Basin, and in the Mersa Matruh gyre and its associate train of anticyclonic gyres extending into the Shikmona gyre.The heat content, as defined above, of the Rhodes gyre is about five times smaller than the heat excess stored in some of the anticyclonic convergence regions. Frontal regions encircling the major gyres are easily identified in the regions of strong heat content gradients.

The negative salt anomaly (Fig. 22b) characterizing the distribution of AW indicates its diminishing influence within the Rhodes gyre, which is separated by a sharp front from the pool of AW in the southwest. AW influence is found to extend eastwards from the southern side of the Cretan Passage, to become entrapped in the Mersa Matruh gyre which advects it further to the northeast. It is then advected southeastwards to become entrained in the Shikmona gyre. A small part of this water penetrates into the northern region of the Levantine Basin by encircling the Rhodes cyclone and its extension in the form of filaments described earlier. The general distribution of AW inferred from this figure reflects its advection and mixing, influenced by the near-surface circulation.

The distribution of the positive salt anomaly which characterizes LIW distribution is given in Fig. 22c. It is mainly concentrated in anticyclonic eddies in the Gulf of Antalya, and south of Cyprus. It vanishes completely near the centre of the Rhodes gyre, but is found in small but significant amounts along the gyre's periphery: near Rhodes Island, in small cells south of Crete, and to the southeast of Rhodes gyre's centre, both bordering and within the Mersa Matruh gyre.

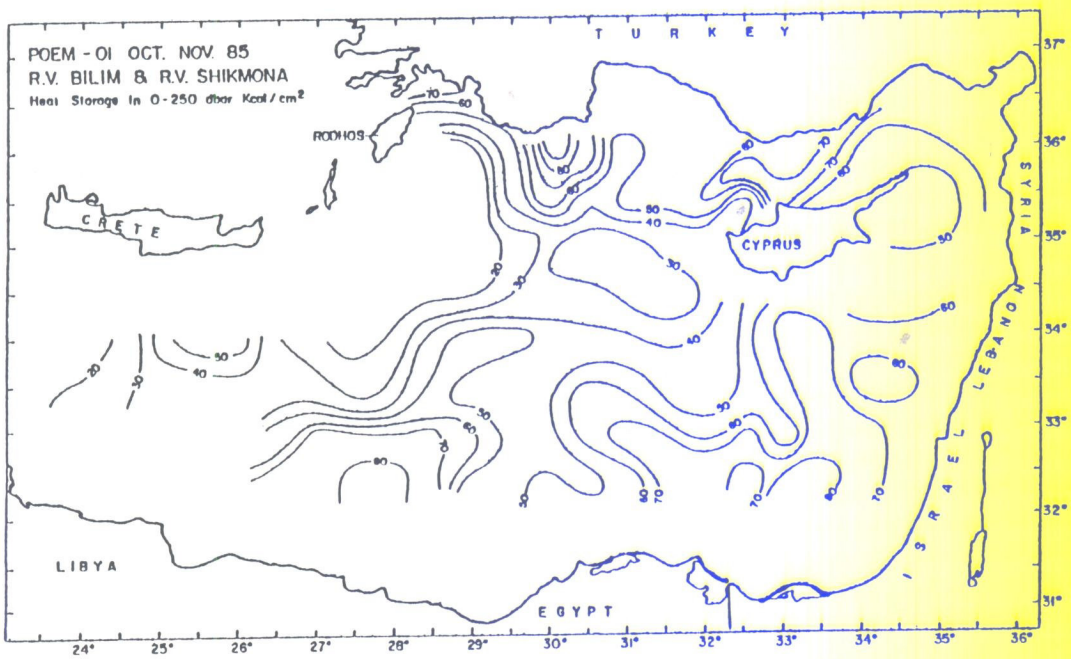

FIG.22a. Heat storage in units of kcal cm^{-2} within the 0-250 dbar layer, calculated relative to a reference temperature of 15°C, ON85.

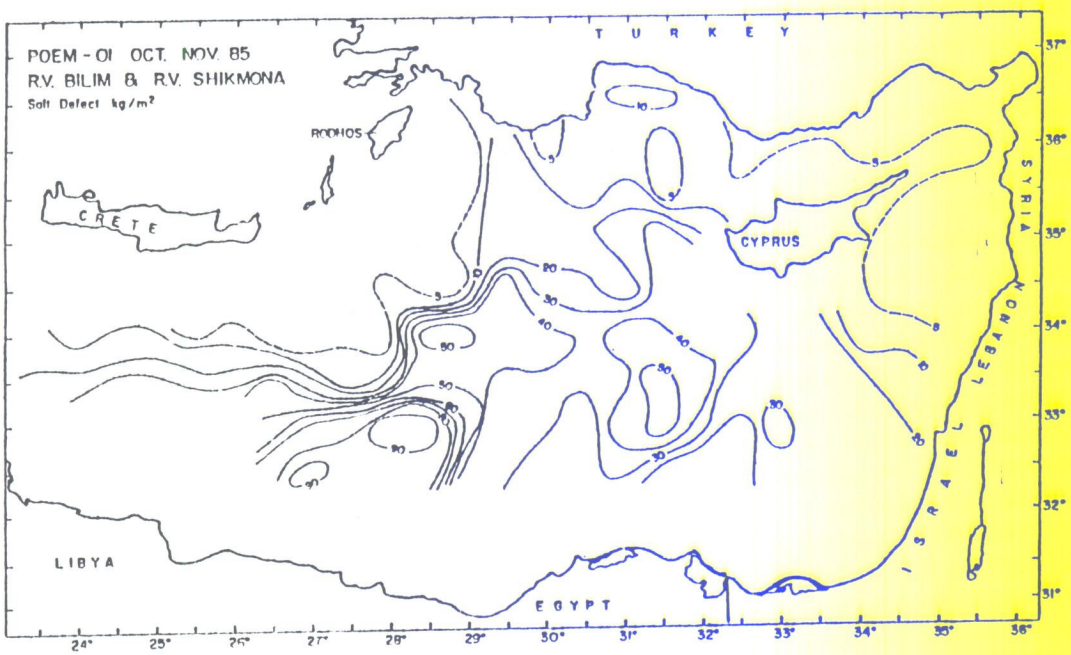

FIG.22b. Negative salt anomaly in units of kg m^{-2} calculated relative to a salinity upper limit of 39.1, ON85.

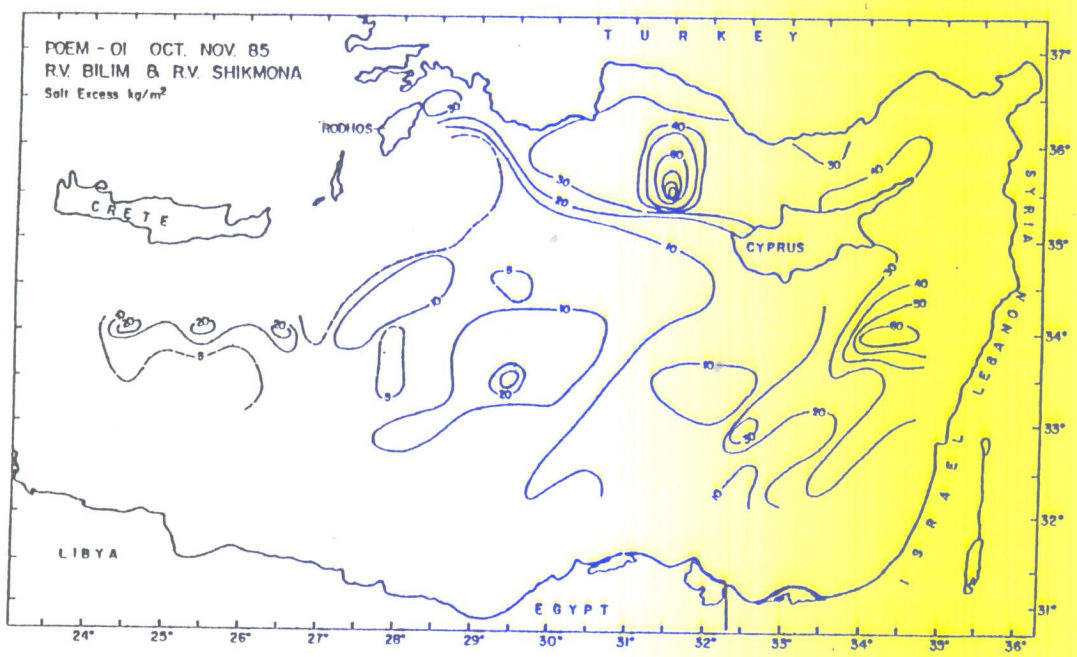

Fig.22c. Positive salt anomaly in units of kg m^{-3} calculated relative to a salinity lower limit of 38.9, ON85.

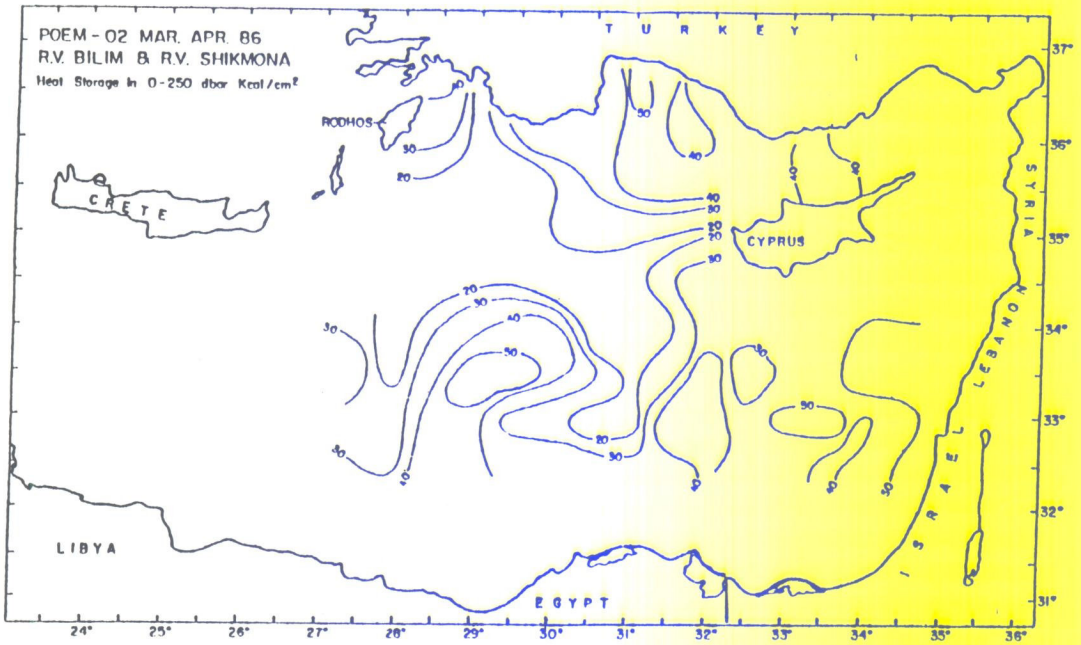

Fig.23a. Heat storage in units of kcal cm^{-2} within the 0-250dbar layer, calculated relative to a reference temperature of 15°C, MA85.

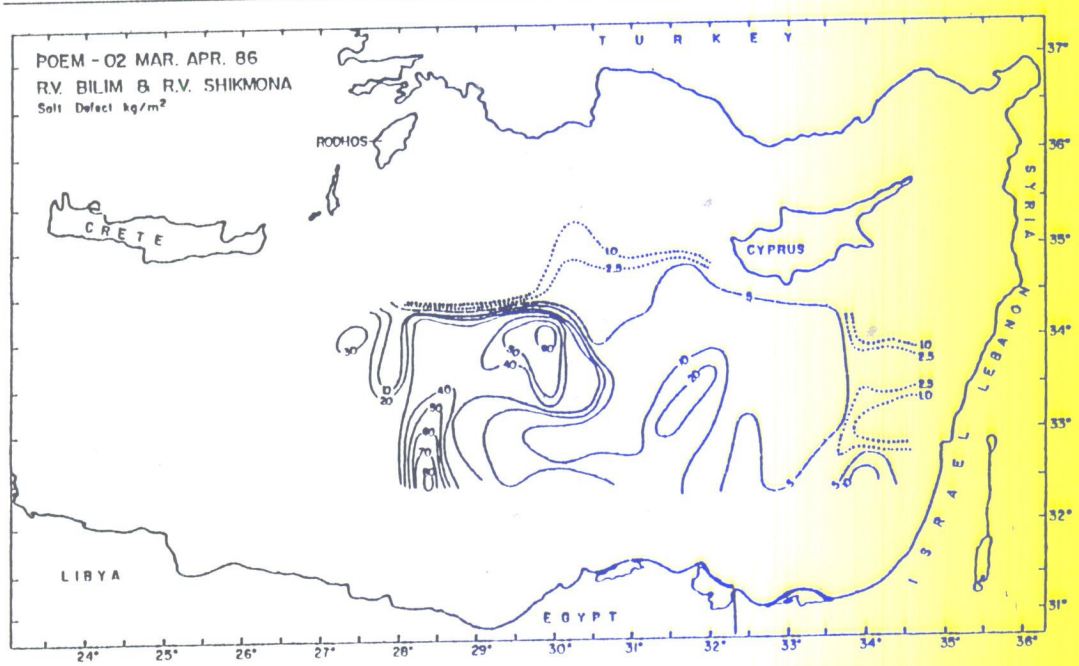

Fig.23b. Negative salt anomaly in units of kg m^{-3} calculated relative to a salinity upper limit of 39.0, MA86.

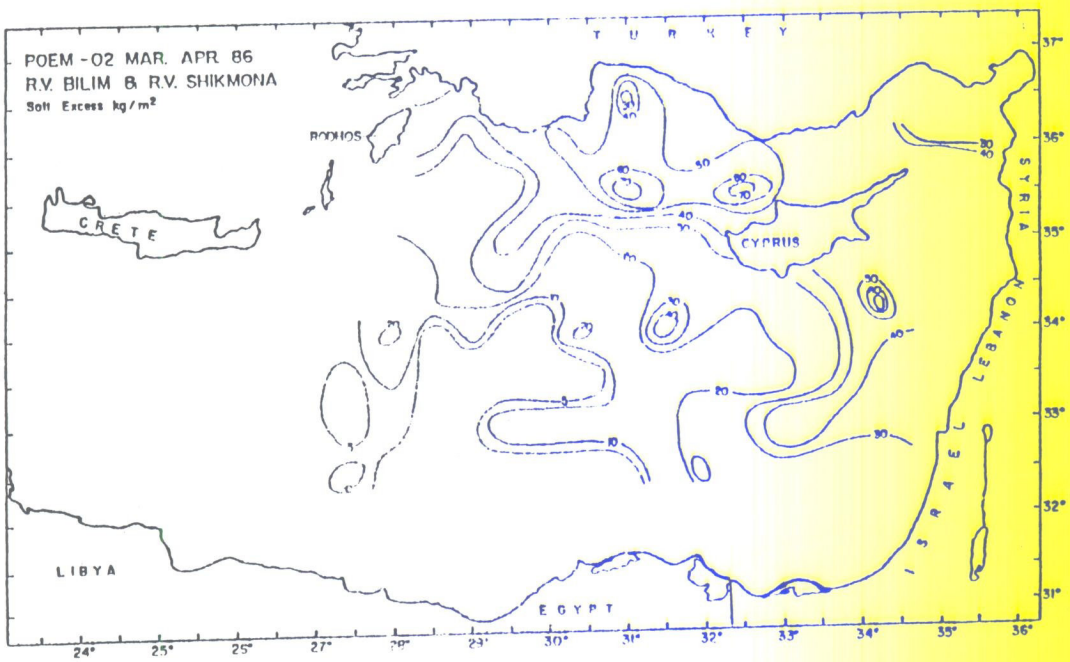

Fig.23c. Positive salt anomaly in units of kg m^{-3} calculated relative to a salinity lower limit of 38.9, MA86.

7.2. *MA86*

Figure 23a shows that the wintertime minimum of heat storage was in the crescentic Rhodes circulation, and its maxima was in the Mersa Matruh, Shikmona and Antalya anticyclonic centres. The AW salt anomaly (Fig.23b) has two maxima within the Mersa Matruh gyre, spreading partially east. A sharp frontal boundary on its northeastern periphery limits the AW stored in this gyre. Extensive mixing, either disperses AW completely or breaks it up into small pockets in the northern Levantine, so computation of AW volumes in this region gives negligible results.

In this survey LIW again is mainly found occupying the northeastern corner of the Basin (Fig.23c), and appears in small anticyclonic cells along the outer periphery of the crescentic Rhodes circulation. Some smaller patches are also observed along the inner periphery. The volume of LIW becomes negligible within the Mersa Matruh gyre.

8. CONCLUSIONS

The results obtained from these two medium resolution surveys highlight the great variability in the circulation and hydrography of the Levantine Basin. Comparisons between the results of the two surveys not only reflect important structural seasonal variability but also confirm the existence of persistent features. Nonlinearities and secular climatological changes can be expected to lead to interannual variability in the patterns presented. The recent observations within the POEM programme represent the first extensive coverage of the whole Levantine Basin region and have provided new insights and understanding, which should be further improved through continuing studies.

Both in the summer and the winter, a number of quasi-permanent sub-basin scale gyres seem to be of central importance in controlling the general circulation and its evolution in time. The Central Levantine Basin Current enters the Basin as a continuation of the North African Current and as a free jet flow detached from the coasts. From then on, it passes in between the major cells of circulation (the Rhodes and Mersa Matruh gyres) and bifurcates into smaller veins in the east, where it partially becomes incorporated into the eddy field. It is only in the northern part of the Basin that the currents gradually become reorganized to form the Asia Minor Current. This current is initially masked by the eddy field along the Anatolian coast in the Cilician Basin but becomes more coherent along the northern periphery of the Rhodes gyre and the shelf slope adjoining the Cretan Archipelago. The cyclonic circulation of the Rhodes gyre occupies an extensive area in the north of the Basin. On the other hand, the Mersa Matruh and Shikmona gyres, and part of the Central Levantine Basin Current make up a complex pattern of mainly anticyclonic circulation in the southern Basin.

In general the main features of the circulation are in agreement with previous descriptions but greater detail has emerged of the occurrence of multiple scales of motion, vertically variable structure, interacting eddies, fronts and jets. The earlier descriptions of the general circulation seriously underestimated the area covered by anticyclonic gyres especially in the southern part of the Levantine Basin where these gyres generate clockwise currents along the southeastern coast.

The sub-basin scale gyres are found not to be homogeneous masses but rather are composed of medium-sized eddies whose extent and internal structure are changing continuously. In a basin as small as the Levantine Basin, the geometrical constraints alone will inhibit the circulation entities from behaving independently. They strongly interact with each other, with the basin and island boundaries and with the bottom topography, hence contributing continually to basin-scale turbulence. Even the sub-basin scale gyres are in close contact with each other, their

extensions often hugging one another. There is considerable vertical variation in the intensity and position of the eddy centres, in association with the baroclinic energy available to these systems. The anticyclonic eddies are generally more persistent with increasing depth. Some of these anticyclonic eddies intensify and split into multiple centres, or two neighboring eddies may interchange their roles with depth, suggesting mergers of these features may be occurring.

Within the Rhodes cyclonic dome upwelling processes tend to homogenize water properties. This leads to the surface waters at the gyre's centre to become exposed to surface effects and mixing. On the other hand, water masses with distinctive properties are both advected by and entrained within the circulatory features. Neither of the distinctive water types appear as coherent or uniform patches. AW enters through the Cretan Passage and can be traced following the main route of the Central Levantine Basin Current; occasionally it 'escapes' through the eddy field into the other domains. The LIW is locally generated, especially in the northeastern sector of the Basin and along the periphery of the Rhodes gyre. Along the northern boundary, it is trapped between the coast and the major cyclonic gyre. At other locations along the periphery of the Rhodes gyre, small patches seem to be sinking so that LIW ends up in the deeper levels of the surrounding anticyclonic eddies.

The sinking motions of LIW were observed to occur in summer as well as in winter, suggesting that the LIW may be maintained continuously in the Levantine Basin, although possibly being formed much more intensely in the peak of winter. The persistent preconditioning of the near-surface waters at the center of Rhodes gyre, the fact that LIW is always characterized with relatively warmer temperatures than the coldest surface temperatures of the winter season, together with the fact that we have found downwards displaced patches of LIW at the Rhodes gyre periphery and intercepted near the coast seem to favour isopycnal processes as being responsible in the LIW formation as well as purely vertical mixing mechanisms.

9. ACKNOWLEDGEMENTS

The R/V *Bilim* surveys were supported by TÜBİTAK, the Turkish Scientific and Research Council, under a monitoring project. We are greatly indebted to the crews of the R/V *Bilim* and the R/V *Shikmona* and to their skippers E. TEZER and A. BEN-NUN respectively, for the efficient use of their technical skills and enduring collaboration. We particularly thank T. OĞUZ, M.A. LATIF, F. BINGEL and C. SAYDAM, scientists of the IMS-METU and J. BISHOP, Z. ROSENTROUB and S. BRENNER, scientists of the IOLR, and similarly express our indebtedness to graduate assistant S. BEŞIKTEPE of the IMS-METU and the technical staff S. BROKMAN, J. MOUWES, R. SELA and M. UDEL of the IOLR whose hard work, support and patience made our endeavours feasible. Our thanks are also due to N. KAVANOZ of the IMS-METU and H. BERNARD of the IOLR for their careful and painstaking drafting of the figures. We express our thanks to E. TZIPERMAN of the Weizmann Institute of Science, Israel for his kind preview and suggestions.

We are also deeply indebted to Prof. A.R. ROBINSON and Prof. P. MALANOTTE-RIZZOLI who were instrumental in the organization of the coordination of the POEM cruises. The major part of this work was completed during a visit to the IMS-METU by A. HECHT, with financial support from the IOLR.

10. APPENDIX A — DATA PROCESSING

Initial data processing and quality control were carried out separately on the two data sets:

The SBE-CTD data were initially averaged *in situ* every consecutive 1 second period (hardware decimating averages). The noise in the pressure signal was reduced by filtering it three times by an equivalent triple point moving average

filter (triple least squares fitting). Logical quality checks based on allowed limits of the measured parameters and their vertical gradients, on CTD lowering speed and acceleration and on density inversions led to the elimination of some additional data. The data were also run through a despiking median filter with a window length of 5 data points. The processing details are reported in ÖZSOY, OĞUZ, LATİF and ÜNLÜATA (1987).

The NB-CTD data were corrected for the time constant of the temperature sensor (FOFONOF, HAYES and MILLARD, 1974) and then smoothed with a 10 point decimating average. The resulting data were bin-averaged in 1 db bins, standard deviations (σ) for each bin were computed, data exceeding a 2σ range were eliminated and the bin average recomputed. Further corrections for the NB-CTD were carried out with calibration factors computed from independent measurements of temperature, salinity and pressure which were acquired by a rosette sampler at 6 to 12 levels during each CTD cast. The visual inspection of the vertical profiles of temperature, of the salinity and of the S/T diagrams indicated additional doubtful data points which were inspected and weeded out if necessary.

For time intervals of the order of a few days and distances of the order of 10km, the water mass properties below 500m throughout most of the Levantine Basin are almost constant. This consistency was used to monitor the accuracy and the repeatability of the CTDs as well as to provide intercalibration between the two data acquisition systems. The comparisons of data obtained on casts separated by a few hours to a few days indicated that the repeatability of the NB-CTD was 0.01°C and 0.03 for salinity and that of the SBE-CTD was 0.01 °C and 0.01 for salinity. Measurements at the intercalibration station (34°00'N, 31°30'E) indicated that there was a disparity between the two instruments of +0.04 °C and +0.03 in salinity (SBE-CTD values being smaller as compared to NB-CTD) during the ON85 experiment and +0.02°C and +0.06 in salinity during the MA86 respectively. Since only the NB-CTD had been calibrated independently a correction ~~factor~~ was applied to the SBE-CTD. However, the differences between the two systems were small especially in terms of density differences ($\delta\sigma_t$) between the two data sets since both the temperature and the salinity corrections were positive.

All the relevant oceanic parameters were computed with the standard routines of FOFONOFF and MILLARD (1983).

APPENDIX B — DATA ANALYSIS

The objective analysis of the geopotential anomaly followed the algorithm of BRETHERTON, DAVIS and FANDRY (1976), using the version with an estimated mean of the field. Although the geopotential anomaly field has a zero mean, this feature becomes particularly important when using the approach of CARTER (1983), where the analysis is computed from the nearest observations within a predetermined radius of influence. In fact, this approach accounts for the large scale variations (trends) in the observed field and therefore the mean of the observations should be properly estimated. A homogeneous, isotropic correlation function was assumed and it was modelled as

$$C(r) = (1 + a_2 r^2 + a_3 r^3)\exp(-br^2) \qquad \text{(A1)}$$

where the polynominal terms are truncated at third power and the linear term has been omitted ($a_1 = 0$) by requiring a vanishing gradient at zero lag (real wave number spectrum). The exponential term attenuates the influence of distant

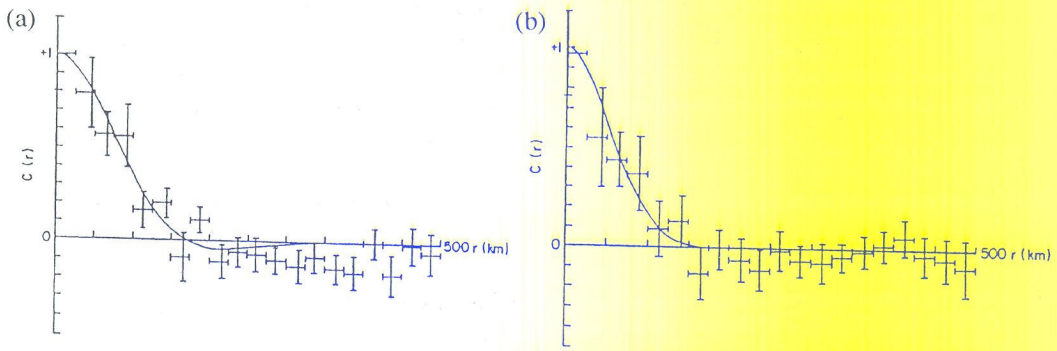

FIG.A1a,b. The experimental correlations showing the 90% confidence limits and the least squares fitted model for surface geopotential anomaly, (a) ON85, (b) MA86.

observations, hence that of unstable correlation estimates (CARTER, 1983). The decay coefficient in (A1) was determined so as to yield an exponential term of 0.05 at one quarter of the largest distance between the observations. The homogeneous isotropic model was selected because of the small sample size, which however, was large enough to allow the computation of the polynominal coefficients by least squares fitting of the model. The inspection of the experimental correlations (Figs. A1a and b) led us to select a radius of influence of 200-250km and limit our computations to the contribution of the nearest 12 points. A normalized error variance of ϵ=0.1 (BRETHERTON *et al.*, 1976)

(a)

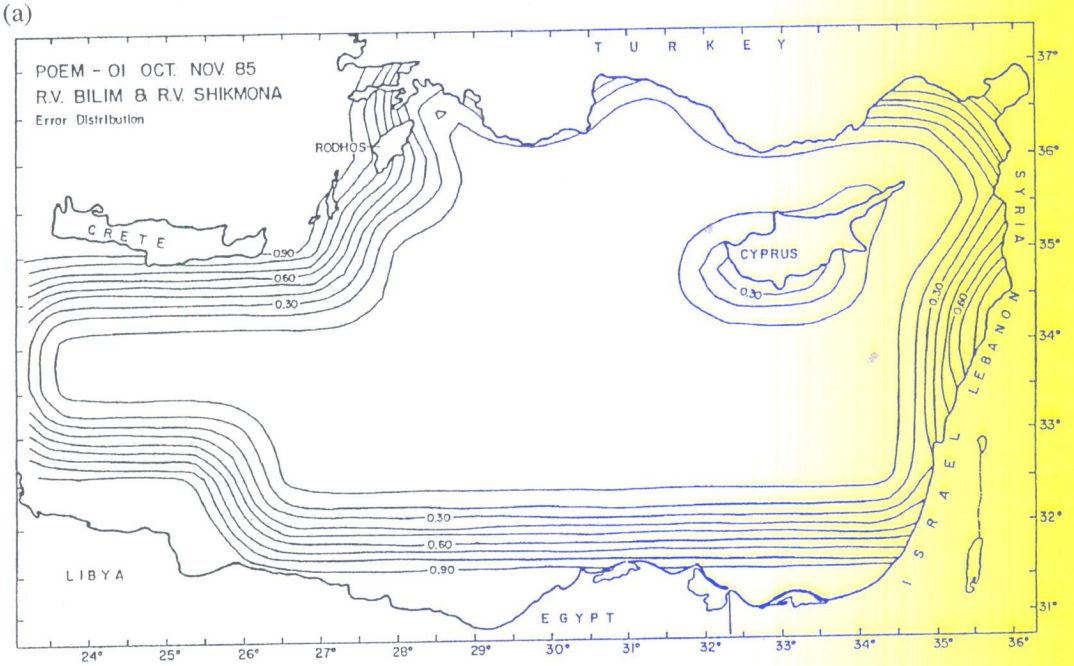

(b)

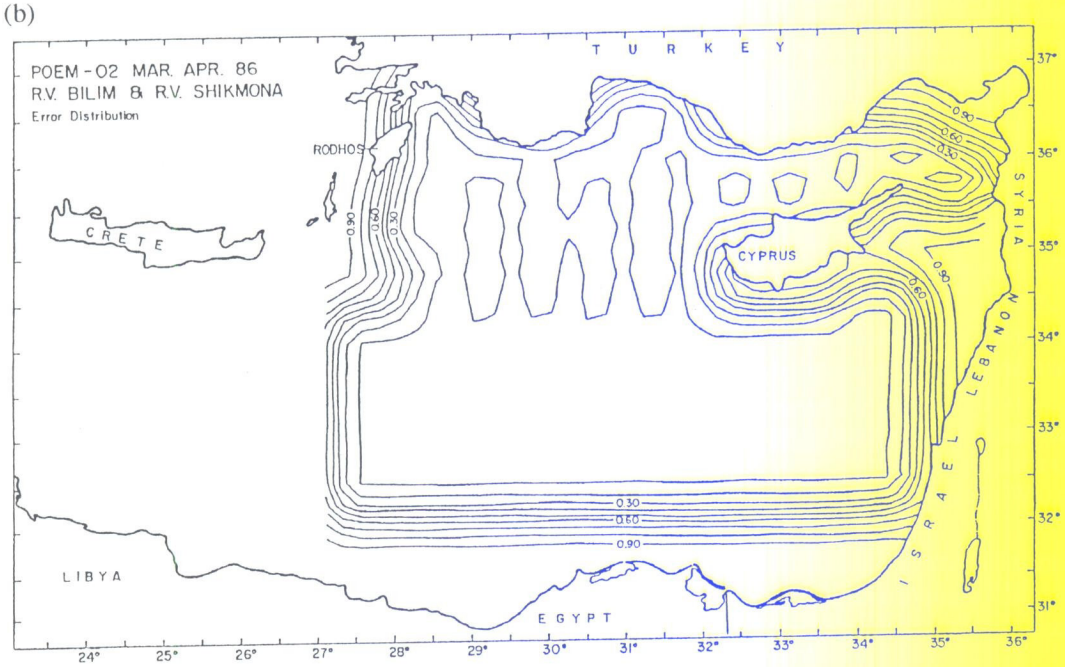

FIG.A2a,b. Error variance maps of the objective analysis of the sea surface dynamic topography (normalized by the total observational variance) ***based on the data from both ships, (a) ON85, (b) MA86.

was used in the analysis.

The validity of the quasi-synoptic combination of the two data sets was tested by running independent objective analyses of each of them and then comparing the resulting topographies of the geopotential anomaly of the surface layer. The chosen reference level was the same for both data sets but the correlation models were determined separately by each of the data sets. The sign, magnitudes and orientations of the streamlines on both sides of the common boundary at 34°30'N latitude coincided reasonably well with each other (results not shown here), thus encouraging the combination of the two data sets. The combined data set was used to compute the geopotential anomaly at 0, 30, 50, 80, 100, 200, 300, 400, 500, and 600db relative to reference level at 800db. The error variance distribution map (e.g. Fig. A2a and b) shows the uniformity of the estimates throughout the basin, with the exception of those regions where we did not have the necessary information, i.e. the Cretan Arc, south of Cyprus, near the coasts of Lebanon, Libya and Egypt and in the shallow Gulf of Iskenderun. The topography of the surface geopotential anomaly resulting from the objective analysis of the combined data set (e.g. Fig.3a) shows the smooth blending of the data and demonstrates the negligible sensitivity of the analysis to the time gap between the two data sets.

Some of the most conspicuous features of the geopotential map (Fig.3a) are the streamlines that cross the coastlines. These could be attributed to ageostropic processes on the continental shelf (e.g. downwelling — O VCHINNIKOV, 1966; topographic Rossby waves — ÜNLÜATA, 1982) and to the non-synoptic nature of the data, but are equally likely to be artefacts of the analysis. One method of forcing the analyses to obey coastal boundaries is to insert streamfunction values on the coasts (A. ROBINSON, personal communication), however, there is no way to an independent determination of these values. This method was first implemened (although the results are not presented here for reasons of limited space) by averaging objectively projected values with error below a specified limit along the coasts of the mainland and the various islands to determine 'along the coast' streamlines. The objective analysis was then constrained to comply with these values. The results were not satisfactory, since the method produced an unreasonable anticlockwise circulation along the mainland Levantine coast. This appears to result mainly from the many anticlockwise eddies which are generally closer to the coast than the cyclonic ones. Better results, in this respect, were obtained by forcing the objective analysis to comply with subjectively extrapolated coastal values. In this case, the error distribution was improved, but did not seem to change significantly the geopotential anomaly map except in the coastal regions which were arbitrarily modified in the first place. Thus, between the two methods, the one being overly restrictive and the other being subjective, we chose to ignore the influence of the coast altogether.

12. REFERENCES

ACCERBONI, E. and G. GRANCINI (1972) Measurés Hydrologiques en Mediterranèe Orientale (Septembre 1968) *Bolletino di Geofisica Teoretica ed Applicata*, **14** (53-54), 24pp.

ANATI, D.A. (1984) A Dome of Cold Water in the Levantine Basin. *Deep-Sea Research*, 31 (10), 1251-1257.

ARHAN, M. (1987) On the Large Scale Dynamics of the Mediterranean Outflow. *Deep-Sea Research*, **34** (7), 1187-1208.

BETHOUX, J.P. (1979) Budgets of the Mediterranean Sea. Their Dependence on the Local Climate and on the Characteristics of the Atlantic Waters. Oceanologica Acta, **2**, (2), 157-164.

BETHOUX, J.P. (1980) Mean Water Fluxes Across Section in the Mediterranean Sea, Evaluated on the Basis of Water and Salt Budgets and of Observed Salinities. *Oceanologica Acta*, **3**, 79-88.

BRETHERTON, F.P., R.E. DAVIS and C.B. FANDRY (1976) A Technique for Objective Analysis and Design of Oceanographic Experiments Applied to Mode-73. *Deep-Sea Research*, **2**, 559-582.

BRODY, L.R. and M.J.R. NESTOR (1980) *Regional Forecasting Aids for the Mediterranean Basin, Handbook for Forecasters in the Mediterranean*, Part 2, Naval Environmental Prediction Research Facility, Monterey, California, Technical Report TR 80-10, 178pp.

BUNKER, A.F. (1972) Wintertime Interactions of the Atmosphere with the Mediterranean Sea. *Journal of Physical Oceanography*, **2**, 225-238.

BUNKER, A.F., H. CHARNOCK and R.A. GOLDSMITH (1982) A Note on the Heat Balance of the Mediterranean and Red Seas. *Journal of Marine Research*, **40** Supplement, 73-84.

CARTER, E.F. (1983) *The Statistics and Dynamics of Ocean Eddies*. Ph.D. thesis, Division of Applied Sciences, Harvard University.

COLACINO, M. and L. DELL'OSSO (1975) The Monthly Heat Budget Isolines on the Mediterranean Sea. *Archiv für Meteorogie Geophysik und Bioklimatologie*, Springer-Verlag, New York, *Ser. A.*, **24**, 171-178.

COLACINO, M. and L. DELL'OSSO (1977) Monthly Mean Evaporation Over the Mediterranean Sea. *Archiv für Meteorogie Geophysik und Bioklimatologie*, Springer-Verlag, New York, *Ser. A.*, **26**, 283-293.

DKSHOD (Turkish Navy Department of Navigation, Hydrography and Oceanography) *Turkish Data Report, Joint Eastern Mediterranean Survey*, NATO Subcommittee on Oceanographic Research, 14pp, Istanbul, 1969.

DZHIOYEV, T.Z. and V.N. DROZDOV (1977) Computation of Stationary Currents in the Eastern Mediterranean Sea. *Oceanology*, 17 (1), 17-19.

EL-GINDY, A.H. and S.H. SHARAF EL-DIN (1985) Water Masses and Circulation in the Deep Layer of the Eastern Mediterranean, Oceanologica Acta, **9**, 239-248.

ENGEL, I. (1967) Currents in the Eastern Mediterranean. *International Hydrographic Review*, **44**, 23-40.

FELIKS, Y. and S. ITZIKOWITZ (1987) Movement and Geographical Distribution of Anticyclonic Eddies in the Eastern

Levantine Basin. *Deep-Sea Research*, **34** (9A), 1499-1508.

Fofonoff, N.P., S.P. Hayes and R.C. Millard Jr. (1974) *WHOI/Brown CTD Microprofiler: Methods of Calibration and Data Handling*. Woods Hole Oceanographic Institution, WHOI Technical Report No. 74-89, 64pp.

Fofonoff, N.P. and R.C. Millard, Jr. (1983) *Algorithms for the Computation of Fundamental Properties of Seawater*, UNESCO Technical Paper in Marine Science 44, 53pp.

Gerges, M.A. (1977) Numerical Investigation of the Circulation in the Mediterranean Sea. Rapports et Proces-Verbaux des Réunions. *Commission Internationale pour l'Exploration Sciantifique de la Mer Méditerranee*, **24** (2), 25-30.

Guibout, P. (1972) *Project Eastern Mediterranean. Results of hydrographic and current measurements on Board the N/O "Jean Charcot", (15 August - 15 September 1967), and results of current measurements on Board the Turkish Frigate "Carsamba"* (1 September - 1 October 1968), NATO Oceanographic Subcommittee, NATO Technical Report No. 68, 89pp., Paris.

Grillaki, D. and S. Piaczek (1985) Numerical Simulations of the Circulation of the Eastern Mediterranean. *NATO SACLANT ASW Research Centre, SACLANTCEN* Report SR-92, 24pp.

Hecht, A., Z. Rosentroub and J. Bishop (1985) Temporal and Spacial Variations of Heat Storage in the Eastern Mediterranean. *Israel Journal of Earth Sciences*, **34**, 51-64.

Hecht, A. (1986) The Hydrology and the Water Masses of the Eastern Mediterranean Sea In: *Proceedings of a UNESCO/IOC First POEM Workshop, Erdemli-Icel, Turkey*, 1986. Part 2, A.R. Robinson and P. Malanotte-Rizzoli editors, POEM Scientific Reports No.1, Cambridge, Mass.

Hecht, A., N. Pinardi and A. Robinson (1988) Currents, Water Masses, Eddies and Jets in the Mediterranean Levantine Basin. *Journal of Physical Oceanography*, 18, 1320-1353.

Hopkins, T. (1978) Physical Processes in the Mediterranean Basins In: *Estuarine Transport Processes*, B. Kjerfve, editor, Columbia, S.C., University of South Carolina Press, 269-310.

Katz, E.J. (1972) The Levantine Intermediate Water Between the Strait of Sicily and the Strait of Gibraltar. *Deep-Sea Research*, **19**, 111-520.

Lacombe, H. and P. Tchernia (1960) Quelques Traits Generaux de l'Hydrologie Mediterranee, *Cahiers Oceanographiques*, **12**, 527-547.

Lacombe, H. and P. Tchernia (1974) *Hydrography of the Mediterranean, Consultation on the Protection of Living Resources and Fisheries from Pollution in the Mediterranean*, FAO, FID;PPM/73/Inf.3, Rome.

May, P.W. (1982) *Climatological Flux Estimates in the Mediterranean Sea: Part I. Winds and Wind Stresses*. Naval Ocean Research and Development Activity, NORDA Report, 54, 56pp.

Malanotte-Rizzoli, P. (1986) The general circulation of the Eastern Mediterranean Sea: Modeling In: *Proceedings of a UNESCO/IOC first POEM Workshop, Erdemli-Icel, Turkey, 1986*. Part 2, A.R. Robinson and P. Malanotte-Rizzoli, editors, POEM Scientific Reports no.1, Cambridge, Mass.

Malanotte-Rizzoli, P. and A. Hecht (1988) The General Circulation of the Eastern Mediterranean Sea: A Review of its Phenomenology and Modelling, *Oceanologica Acta* (in press).

Mediteranean Pilot (1976) Hydrographer of the Navy, United Kingdom, 6 edition, volume 5, 171pp.

Menzin, A.B. and L.V. Moskalenko, (1982) Calculation of Wind-Driven Currents in the Mediterranean Sea by the Electrical Simulation Method (Homogeneous Model), *Oceanology*, **22**, 537-540.

Middelandse Zee (1957) *Oceanographic and Meteorological Data*, Koninklijke Nederlands Meteorologisch Instituut, 91pp.

Miller, A.R., P. Tchernia H. Charnock and D.A. McGill (1970) *Mediterranean Sea Atlas of Temperature, Salinity, Oxygen Profiles and Data from Cruises of R/V Atlantis and R/V Chain with Distribution of Nutrient Chemical Properties*, Woods Hole Oceanographic Institution, Woods Hole, Massachusetts, 190pp.

Morcos, S.A. (1972) Sources of Mediterranean Intermediate Water in the Levantine Sea In: *Studies in Physical Oceanography: a Tribute to G Wust on his 80th Birthday*, editor A.L. Gordon, **2**, Gordon and Breach, New York, 185-206.

Morcos, S.A. and H.M. Hassan (1976) The Water Masses and Circulation in the Southeastern Mediterranean. *Acta Adriatica*, **18**, 195-218.

Mosetti, F., E. Accerboni and A. Lavenia (1972) Recherches Océanographiques en Méditerranée Orientale (Août 1967), *Rapports et Proces-Verbaux des Réunions. Commission Internationale pour l'Exploration Scientifique de la Mer Méditerranée*, **20**, 623-625.

Moskalenko, L.V. (1974) Steady-State Wind-Driven Currents in the Eastern Half of the Mediterranean Sea. *Oceanology*, **14**, 491-494.

Navarra, A. (1986) Surface Fluxes and Air Sea Interaction. In: *Proceedings of UNESCO/IOC First POEM Workshop, Erdemli-Icel, Turkey, 1986*. Part 2, A.R. Robinson and P. Malanotte-Rizzoli, editors, POEM Scientific Reports No.1, Cambridge, Mass.

Nielsen, J.N. (1912) Hydrography of the Mediterranean and Adjacent Waters, In: *Report of the Danish Oceanographic Expedition 1908-1910 to the Mediterranean and Adjacent waters*, **1**, 72-191, Copenhagen.

Nof, D. and L.M. Simon (1987) Laboratory Experiments on the Merging of Nonlinear Anticyclonic Eddies. *Journal of Physical Oceanography*, **17**, 343-357.

Oren, O.H. (1971) The Atlantic Water in the Levant Basin and on the Shores of Israel. *Cahiers Oceanographiques*, **23**, 291-297.

OVCHINNIKOV, I.M. (1965) The Sixth Mediterranean Expedition on the Research Vessel Akademik S. Vavilov. *Oceanology*, **4**, 143-148.

OVCHINNIKOV, I.M. (1966) Circulation in the Surface and Intermediate Layers of the Mediterranean, *Oceanology*, **6**, 48-57.

OVCHINNIKOV, I.M. (1974) On the Water balance of the Mediterranean Sea, *Oceanology*, **14**, 198-202.

OVCHINNIKOV, I.M. (1984) The Formation of Intermediate Water in the Mediterranean, *Oceanology*, **24**, 168-173.

OVCHINNIKOV, I.M. and A.F. FEDOSEYEV (1965) The Horizontal Circulation of the Water of the Mediterranean Sea during the Summer and the Winter Seasons. In: *Basic Features of the Geologic Structure, Hydrological Regime, and Biology of the Mediterranean*, L.M. FOMIN, editor. Translation of the Institute for Modern Languages of the US Navy Oceanographic Office.

OVCHINNIKOV, I.M. and A. PLAKHIN (1965) Formation of Deep Water Masses in the Mediterranean Sea, *Oceanology*, **5**, 40-47.

OVCHINNIKOV, I.M., A. PLAKHIN , L.V. MOSKALENKO, K.V. NEGLYAD, A.S. OSADCHIY, A.F. FEDOSEYEV, V.G. KRISHOVA and K.V. VOYTOVA (1976) *Hydrology of the Mediterranean Sea*, Gidrometeoizdat, Leningrad, 375pp.

OVCHINNIKOV, I.M. and A. PLAKHIN (1984) Formation of the Intermediate Waters of the Mediterranean Sea in the Rhodes Cyclonic Gyre, *Oceanology*, **24**, 317-319.

ÖZSOY, E. (1981) *On the Atmospheric Factors Affecting the Levantine Sea*. European Centre for Medium Range Weather Forecasts, Reading, Berkshire, UK, Technical Report No.25, 29pp.

ÖZSOY, E. and Ü. ÜNLÜATA (1983) Dynamical aspects of the Cilician Basin - Northeastern Mediterranean, NATO Symposium on the Atmospheric and Oceanic Circulation in the Mediterranean, La Spezia, Italy, unpublished manuscript, 46pp.

ÖZSOY, E., C. SAYDAM, I. SALİHOĞLU and Ü. ÜNLÜATA (1986) Sea surface expression of meso-scale eddies in the Northeastern Mediterranean - November 1985, Unesco/IOC First POEM Scientific Workshop, Erdemli, Turkey, 16-20 June 1986. In: *Physical Oceanography of the Eastern Mediterranean (POEM): Initial results*, Unesco Reports in Marine Science, **44**, 92pp.

ÖZSOY, E., M.A. LATİF and Ü. ÜNLÜATA (1986) Meso-scale Hydrographic Characteristics in the Northeastern Mediterranean - November 1985, Unesco/IOC First POEM Scientific Workshop, Erdemli, Turkey, 16-20 June 1986. In: *Physical Oceanography of the Eastern Mediterranean (POEM): Initial Results*. Unesco Reports in Marine Science, **44**, 92pp.

ÖZSOY, E., T. OĞUZ and Ü. ÜNLÜATA (1986) Meso-scale Circulation Features in the Northeastern Mediterranean - November 1985, Unesco/IOC First POEM Scientific Workshop, Erdemli, Turkey, 16-20 June 1986, In: *Physical Oceanography of the Eastern Mediterranean (POEM): Initial Results*. Unesco Reports in Marine Science, **44**, 92pp.

ÖZSOY, E., M.A. LATİF , T. OĞUZ and C. SAYDAM (1986a) Meso-scale Circulation Studies Based on Surveys of 1968 and 1983, Unesco/IOC First POEM Scientific Workshop, Erdemli, Turkey, 16-20 June 1986. In: *Physical Oceanography of the Eastern Mediterranean (POEM): Initial Results*, Unesco Reports in Marine Science, **44**, 92pp.

ÖZSOY, E., M.A. LATİF , T. OĞUZ and C. SAYDAM (1986b) A Note on some Recent Studies of Meso-scale Circulation in the NE Mediterranean, unpublished manuscript, 14pp.

ÖZSOY, E., T. OĞUZ , M.A. LATİF and Ü. ÜNLÜATA (1987) *Ulusal Deniz Ölcme ve Izleme Programi, Akdeniz Alt Projesi, Kuzey Levant Denizi'nin Osinografisi, Cilt 1, Fiziksel Osinografi*, Middle East Technical University, Institute of Marine Sciences, Technical Report, 183pp.

ÖZTURGUT, E. (1976) *The Source and Spreading of the Levantine Intermediate Water in the Eastern Mediterranean*, Saclant ASW Research Centre Memorandum SM-92, La Spezia, Italy, 45pp.

PARMIGGIANI, F., N. PINARDI and G. VIVANTI (1986) Observations of Eddy Variability during POEM-O-85: I) Satellite Sea Surface Temperature Analysis. In: *Proceedings of First POEM Workshop, Erdemli, Turkey, 1986*. Part 2, A.R. ROBINSON and P. MALANOTTE-RIZZOLI, editors, POEM Scientific Reports No.1, Cambridge, Mass.

PEDLOSKY, J. (1979) *Geophysical Fluid Dynamics*, Springer-Verlag, New York, 624pp.

PEIXOTO, J.P., M. de ALMEDIA, R.D. ROSEN and D.A. SALSTEIN (1982) Atmospheric Moisture Transport and the Water Balance of the Mediterranean Sea. *Water Resources Research*, **18**, 83-90.

PHILIPPE, M. and L. HARANG (1982) Surface Temperature Fronts in the Mediterranean Sea from Infrared Satellite Imagery. In: *Hydrodynamics of Semi-Enclosed Seas*, J.C.J. NIHOUL, editor, Elsevier, Amsterdam, 91-128.

PINARDI, N., A.R. ROBINSON and A. HECHT (1986) Process Studies in the Eastern Levantine Basin. In: Proceedings of a UNESCO/IOC First POEM Workshop, Erdemli-Icel, Turkey, 1986. Part 2, A.R. ROBINSON and P. MALANOTTE-RIZZOLI, editors, POEM Scientific Reports No.1, Cambridge, Mass.

REITER, E.R. (1975) *Handbook for Forecasters in the Mediterranean; Weather Phenomena of the Mediterranean Basin; Part 1: General Description of the Meteorological Processes*, Environmental Prediction Research Facility, Naval Postgraduate School, Monterey, California, Technical Paper No. 5-75, 344pp.

REPAPIS, C.C., C.S. ZEREFOS and B. TRITAKIS (1978) On the Etesians over the Aegean. *Praktika Academy of Athens*, **52**, 572-606.

ROBINSON, A.R., Y. FELIKS and N. PINARDI (1983) Process Studies and Dynamical Forecast Experiments for the Eastern Mediterranean, NATO Symposium on the Atmospheric and Oceanic Circulation of the Mediterranean, La Spezia, Italy, unpublished manuscript, 41pp.

Robinson, A.R., A. Hecht, N. Pinardi, J. Bishop, W.G. Leslie, Z. Rosentroub, A.J. Mariano and S. Brenner (1987) Small Synoptic/Mesoscale Eddies and Energetic Variability of the Eastern Levantine Basin. *Nature, London,* **327**, 131-134.

Rosentroub, Z., J. Bishop and A. Hecht (1985) State of the Sea: Physical Aspects, In: *Multidisciplinary Studies of the Eastern Mediterranean 1984-1985.* An Annual Report on Physical, Chemical and Biological Investigations, Israel Oceanographic Limnological Research Ltd., 23-47.

Satmer, Bulletin Mensuel (1983 onwards) La Centre de Meteorologie Spatiale, Lannion, France, No.1 (monthly bulletins).

Schott, G. (1915) Gewasser der Mittelmeeres. *Annalen der Hydrographie u. maritime meteorologie*. **43**, 49-79.

Tziperman, E. and A. Hecht (1988) On the Circulation in the Levantine Basin by Inverse Methods. *Journal of Physical Oceanography*, **18**, (3) 506-518.

UNESCO (1984). *Physical Oceanography of the Eastern Mediterranean: An Overview and Research Plan*, Unesco Reports in Marine Science, **30**, 36pp.

Ünlüata, Ü. (1986) *A Review of the Physical Oceanography of the Levantine and the Aegean Basins of the Eastern Mediterranean in Relation to Monitoring and Control of Pollution*, Institute of Marine Sciences, METU Technical Report, 55pp.

Ünlüata, Ü, Özsoy, E. and M.A. Latif (1980) On the Variability of Currents in the Northeastern Levantine Sea. *Ves Journes Etud. Pollutions*, Cagliari, C.I.E.S.M., 929-936.

Ünlüata, Ü, Oguz, T. and E. Özsoy (1983) Blocking of Steady Circulation by Coastal Geometry. *Journal of Physical Oceanography*, **13**, 1055-1062.

Ünlüata, Ü, Özsoy, E. and M.A. Latif (1986) On the distribution of the Atlantic and the Intermediate Waters in the Levantine, Unesco/IOC First POEM Scientific Workshop, Erdemli, Turkey, 16-20 June 1986. In: *Physical Oceanography of the Eastern Mediterranean (POEM): Initial Results*. Unesco Reports in Marine Science, **44**, 92pp.

Wüst, G. (1961) On the Vertical Circulation of the Mediterranean Sea. *Journal of Geophysical Research*, **66**, 3261-3271.

Zore-Armanda, M. (1969) Water Exchange between the Adriatic and the Eastern Mediterranean. *Deep-Sea Research*, **16**, 171-178.